INFN Angela Bonaccorso
Istituto Nazionale
di Fisica Nucleare
SEZIONE DI PISA

Inpc 2016

Direct Reaction Theory for Exotic Nuclei (RIBs)

- For the plan of the talk please see the book of abstract
- A dedicated conference every second year:

DREB2018, Matsue, Japan

http://conferences.triumf.ca/DREB2016/index.html Halifax

https://indico.gsi.de/conferenceDisplay.py?confId=2347 Darmstadt

http://dreb2012.df.unipi.it/Dreb/WELCOME.html Pisa

Also direct reactions and projectile breakup in particular are important in astrophysics and for practical applications. The International Atomic Energy Agency recently completed a Coordinated Research Project (CRP) to update the Fusion Energy Nuclear Data Library (FENDL).

~300 stable nuclei, ~ 7000 “exotic”

INFN Angela Bonaccorso
Istituto Nazionale di Fisica Nucleare
SEZIONE DI PISA

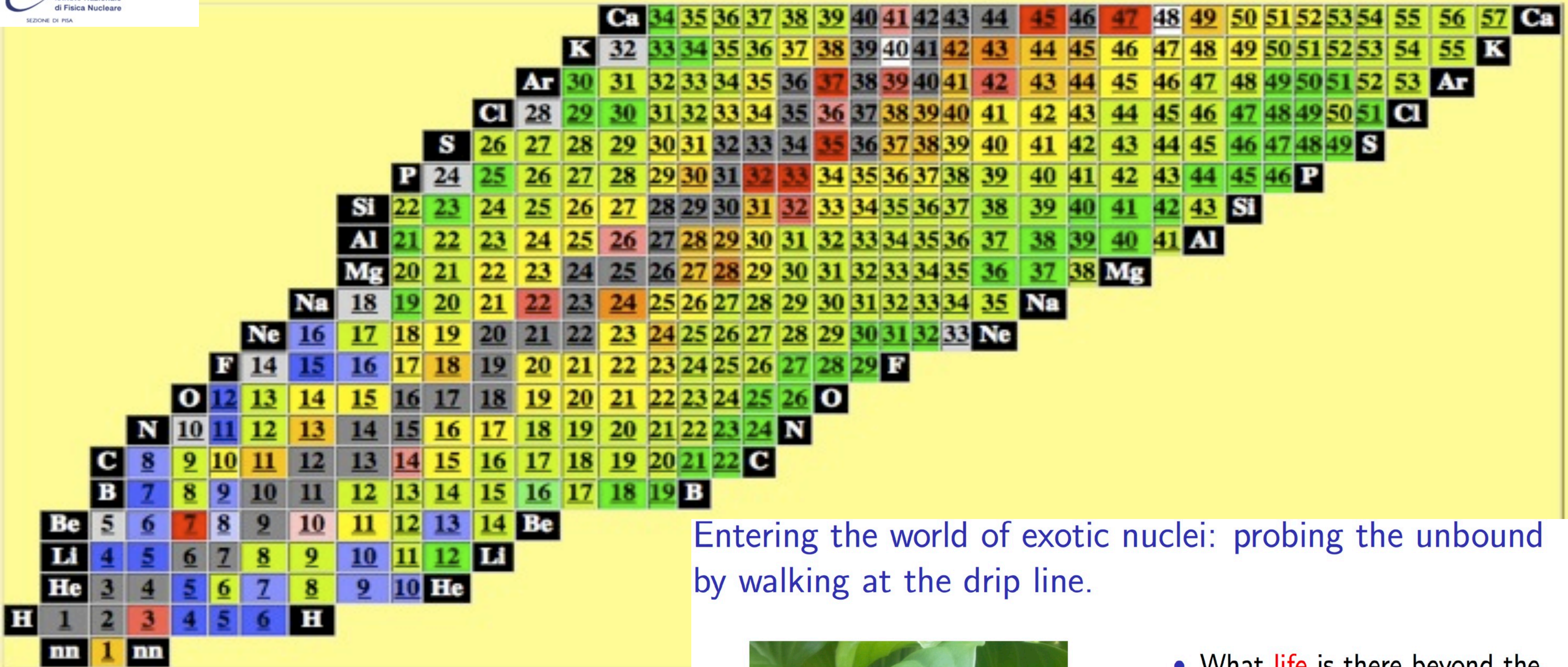

Colour codes:

$< 10^{-21}$ s	10^{-21} - 10^{-18} s
10^{-18} - 10^{-15} s	10^{-15} - 10^{-12} s
1 - 1000 ps	1 - 1000 ns
1 - 1000 ms	1 - 1000 ms
1 - 60 s	1 - 60 m
1 - 24 h	1 - 365 d
1 - 1000 y	10^{3} - 10^{6} y
10^{6} - 10^{9} y	$> 10^{9}$ y
Stable	
Unknown	

Entering the world of exotic nuclei: probing the unbound by walking at the drip line.

- What life is there beyond the dripline?
- How can we discover it without getting lost?
- Extend our understanding of the *residual* nuclear force.
- Check the limits of validity of structure models such as the SHELL MODEL or "ab initio" models.
- Challenges in peripheral reaction theory.

Rewriting Nuclear Physics textbooks
30 years with Radioactive Ion Beam Physics

Pisa (Italy), July 20th – 24th, 2015

Students from all over the world gather together to learn about the wonders of the Physics with Exotic Nuclei

Featuring as special guests

Björn Jonson, Fundamental Physics, Chalmers University of Technology, Göteborg, Sweden
Isao Tanihata, SPANEE and IRCNPC, Beihang University, Beijing, China and RCNP, University of Osaka, Japan

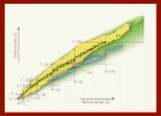

Local Organizing Committee

Angela Bonaccorso, INFN, Pisa (co-chair)
Giovanni Casini, INFN, Firenze (co-chair)
Ignazio Bombaci, Department of Physics, University of Pisa
Laura Elisa Marcucci, Department of Physics, University of Pisa
Alejandro Kievsky, INFN, Pisa
Valeria Rosso, Department of Physics, University of Pisa
Michele Viviani, INFN, Pisa

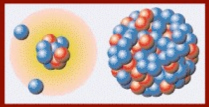

International Coordination Committee

Andrei Andreyev, University of York, UK
Thomas Aumann, University of Darmstadt and GSI, Darmstadt, Germay
Yorick Blumenfeld, IPN, Orsay, France (chair)
Raquel Crespo, IST/C2TN, Lisbon, Portugal
Pierre Descouvemont, ULB, Bruxelles, Belgium
Hans Fynbo, University of Aahrus, Denmark
Nasser Kalantar, KVI – CAR, Groningen, The Netherlands
Rituparna Kanungo, St Mary's University, Halifax, Canada
Adam Maj, PAN, Krakow, Poland
Jie Meng, Peking University, China
Tohru Motobayashi, RIKEN, Japan
Nigel Orr, LPC, Caen, France
Berta Rubio, IFIC, Valencia, Spain
Thomas Nilsson, Chalmers, Gotegorg, Sweden
Lee Sobotka, Washington University, St Louis, USA
Dario Vretenar, University of Zagreb, Croatia

Italian University Coordination Committee

Mauro Bruno, University of Bologna
Francesco Cappuzzello, University of Catania
Maria Agnese Ciocci, University of Siena
Giampaolo Cò, University of Lecce
Giacomo de Angelis, LNL INFN, Legnaro
Domenico Di Bari, University of Bari
Alessandro Drago, University of Ferrara
Carlotta Giusti, University of Pavia
Nunzio Itaco, University of Napoli
Silvia Leoni, University of Milano
Gabriele Pasquali, University of Firenze
Francesco Pederiva, University of Trento
Giovanni Pollarolo, University of Torino
Francesca Rizzo, University of Catania
Giovanni Salmè, INFN, Roma
Elena Santopinto, INFN, Genova
Sergio Scopetta, University of Perugia
Francesca Soramel, University of Padova
Claudio Spitaleri, University of Catania
Andrea Vitturi, University of Padova

Lecture's Editorial Board

Nicolas Alamanos, IRFU, CEA, Saclay, France
Carlos Bertulani, Texas A&M University, Commerce, Texas, USA
Angela Bracco, University of Milano, Italy
David Brink, University of Oxford, UK

Lucia Lilli and Claudia Tofani, INFN, Pisa (Secretaries): ExoticNuclei2015@pi.infn.it
http://exotic2015.df.unipi.it

The image cannot be displayed. Your computer may not have enough memory to open the image, or the image may have been corrupted. Restart your computer, and then open the file again. If the r still appears, you may have to delete the image and then insert it again.

A very happy group of young physicists

INFN Angela Bonaccorso

I.Tanihata, "HOW IT ALL STARTED"

Focus Point
in EPJ+, 131 4 (2016) 90
Re-writing Nuclear Physics textbooks: 30 years of radioactive ion beam physics
DOI: 10.1140/epjp/i2016-16090-x

http://exotic2015.df.unipi.it/

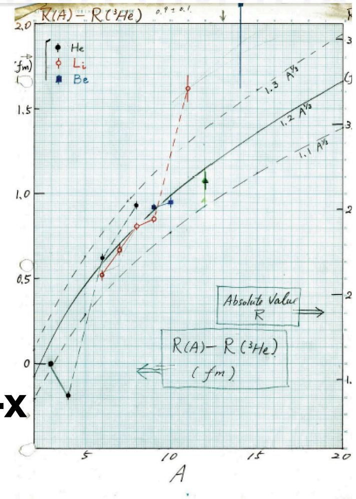

Fig. 11 The firstly determined radii of He, Li, and isotope radii. R in this figure is R_I in the text.

Early experiments: halo nuclei

I. Tanihata et al., Phys. Lett. B 160, 380 (1985)

$$\sigma_I = \pi [R_I(P) + R_I(T)]^2$$

$$\sigma_R = \pi\left(R_{vol} + R_{surf}\right)^2\left(1 - \frac{B_c}{E_{cm}}\right)$$

Kox et al. (1987)

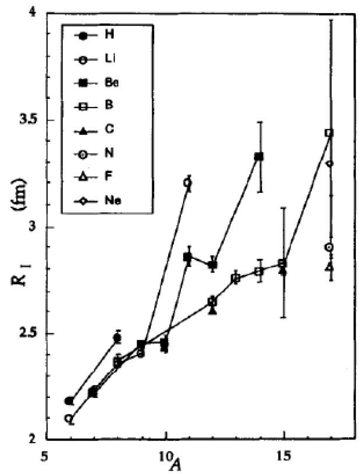

Early theory: halo nuclei
P. G. Hansen and B. Jonson, Europhys. Lett., 4, 409 (1987)

Early eikonal model

I. Tanihata, Prog. Part. Nucl. Phys. 35, 505 (1995)

These equations provide a simple way to compare the reaction cross sections at different energies. However, since they are purely empirical formula, one should be careful when applying them to an exotic nucleus because of a possible difference in the surface diffuseness as well as any proton-neutron density difference. When one measures σ_R using a β-unstable nucleus, only r_0 is expected to change.

$$\sigma_R = \int_0^\infty d\mathbf{b}(1 - |S(\mathbf{b})|^2)$$
$$= \sigma_{ct} + \sigma_{nt}$$

decoupling of core and halo

$$|S(\mathbf{b})|^2 = |S_{ct}|^2 |S_{nt}|^2$$
$$= |S_{ct}|^2 - |S_{ct}|^2 |S_{nt}|^2$$

$$|S(\mathbf{b})|^2 = e^{-[\sigma_{nn} \int ds \rho_p(|b-s|)\rho_t(s)]}$$
$$= e^{-[\sigma_{nn} \int ds \rho_c \rho_t]} e^{-[\sigma_{nn} \int ds \rho_n \rho_t]}$$

$$\sigma_{nt} = \int_0^\infty d\mathbf{b} |S_{ct}|^2 P_{bup}$$

What should we be re-writing about:

at the beginning it was the compound nucleus and resonance theory

- N. Glendenning book
- N. Bohr, Breit & Wigner, Kapur & Peierls, Feshbach & Wisskopf **1936**-1947

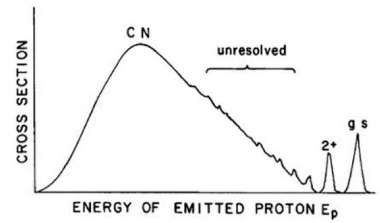

Fig. 1.1. Schematic proton spectrum from proton–nucleus scattering showing resolved levels near the beam energy, unresolved, but discrete, levels, and the com[pound] nucleus continuum.

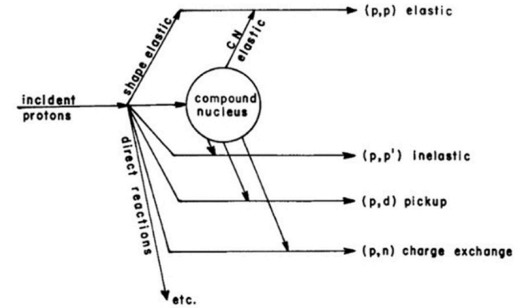

Fig. 1.2. Depiction of the processes that are typical of proton–nucleus interactions. (Adapted from P. E. Hodgson, 1971.)

BUT THEN

- DIRECT REACTION THEORY
- Butler 1950
- Bethe and Butler 1952
- Butler, Austern, Pearson 1958

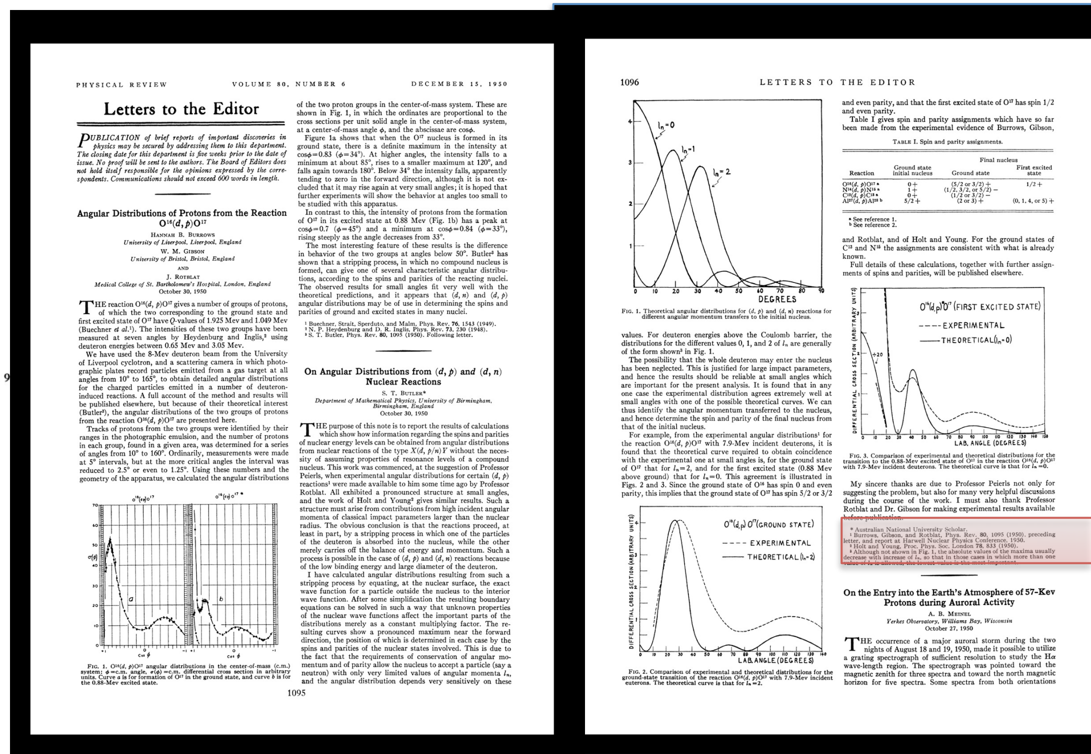

PHYSICAL REVIEW VOLUME 80, NUMBER 6 DECEMBER 15, 1950

Letters to the Editor

Angular Distributions of Protons from the Reaction $O^{16}(d,p)O^{17}$

On Angular Distributions from (d, p) and (d, n) Nuclear Reactions

S. T. BUTLER

LETTERS TO THE EDITOR

On the Entry into the Earth's Atmosphere of 57-Kev Protons during Auroral Activity

PHYSICAL REVIEW VOLUME 112, NUMBER 4 NOVEMBER 15, 19[58]

Semiclassical Treatment of Direct Nuclear Reactions

S. T. BUTLER, N. AUSTERN,* AND C. PEARSON
The F.B.S. Falkiner Nuclear Research and Adolph Basser Computing Laboratories, School of Physics,† The University of Sydney, Sydney, N.S.W., Australia

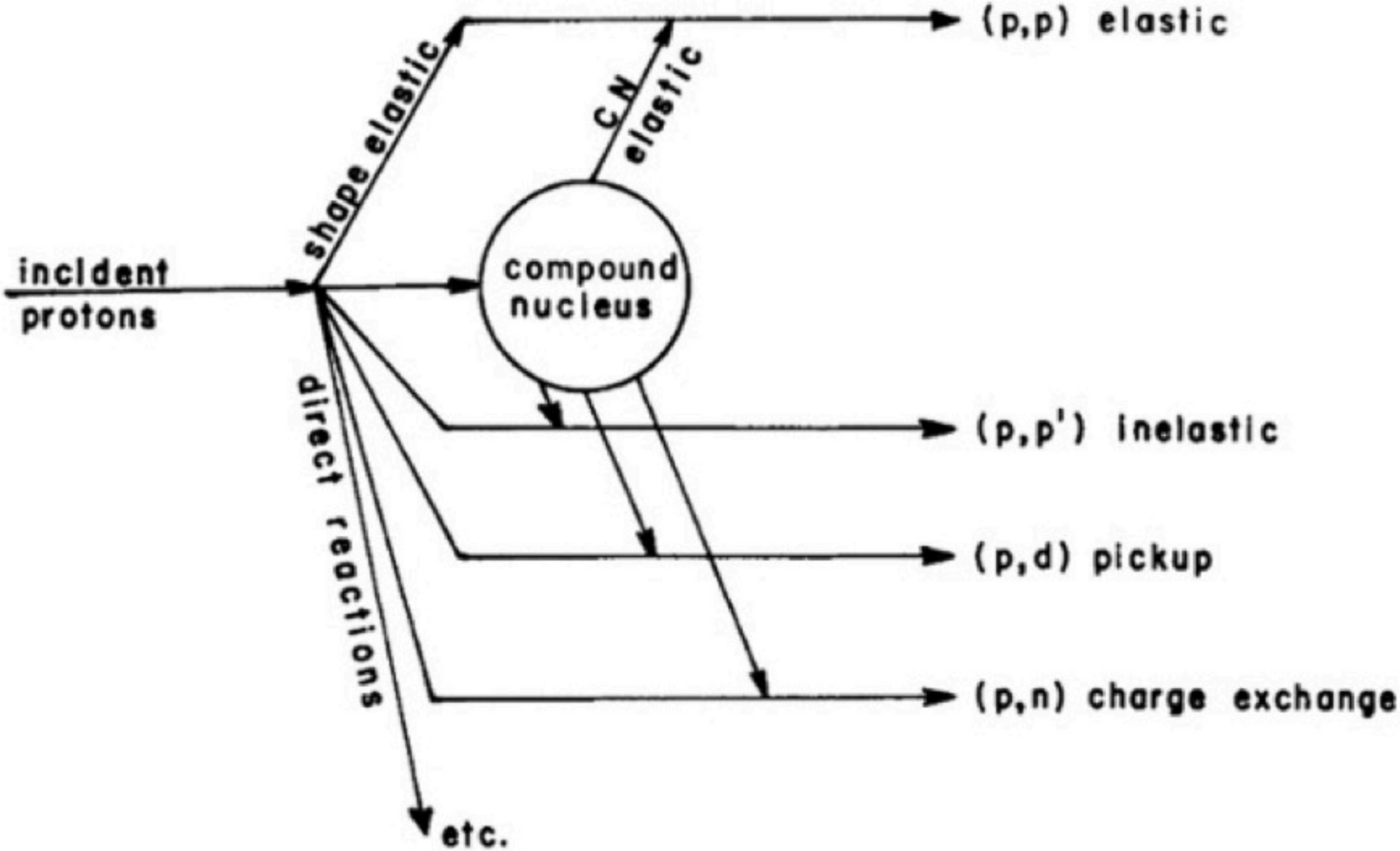

Fig. 1.2. Depiction of the processes that are typical of proton–nucleus interactions. (Adapted from P. E. Hodgson, 1971.)

- Peripherality
- Matching conditions: selectivity
- Weak binding
- Large nuclear dimensions

Spectroscopic information

nucleus. This work was commenced, at the suggestion of Professor Peierls, when experimental angular distributions for certain (d, p) reactions[1] were made available to him some time ago by Professor Rotblat. All exhibited a pronounced structure at small angles, and the work of Holt and Young[2] gives similar results. Such a structure must arise from contributions from high incident angular momenta of classical impact parameters larger than the nuclear radius. The obvious conclusion is that the reactions proceed, at least in part, by a stripping process in which one of the particles of the deuteron is absorbed into the nucleus, while the other merely carries off the balance of energy and momentum. Such a process is possible in the case of (d, p) and (d, n) reactions because of the low binding energy and large diameter of the deuteron.

Angela Bonaccorso

Istituto Nazionale di Fisica Nucleare

SEZIONE DI PISA

Heavier projectiles, higher incident energies

J. Phys. G: Nucl. Phys. 11 (1985) 935–952. Printed in Great Britain

Perturbation approach to nucleon transfer in heavy-ion reactions

L Lo Monaco and D M Brink

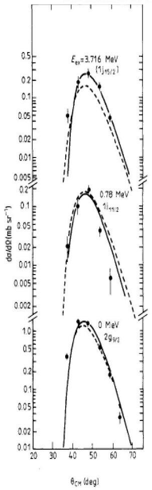

Figure 2. Angular distributions for the ^{208}Pb(^{16}O, ^{15}O)^{209}Pb reaction at 139 MeV. The full curves represent DWBA calculations of Olmer *et al* (1978) while the broken curves are obtained using our formulae.

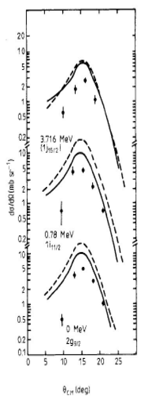

Figure 3. Angular distributions for the ^{208}Pb(^{16}O, ^{15}O)^{209}Pb reaction at 312.6 MeV. The full curves represent DWBA calculations. The broken curves indicate our predictions.

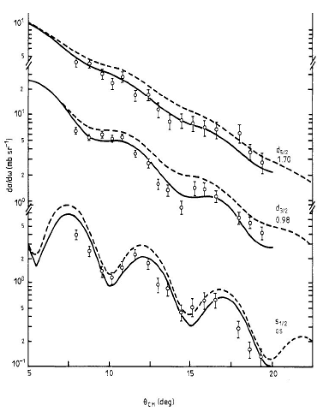

Figure 4. Differential cross sections for the ^{26}Mg(^{11}B, ^{10}B)^{27}Mg reaction at 114 MeV. The DWBA calculations of Paschopoulos *et al* (1975) are indicated by full curves. The broken curves correspond to the present calculation.

J. Phys. G: Nucl. Phys. 13 (1987) 1407–1428. Printed in the UK

Nucleon transfer in heavy-ion reactions: energy dependence of the cross section

A Bonaccorso†, D M Brink‡ and L Lo Monaco‡

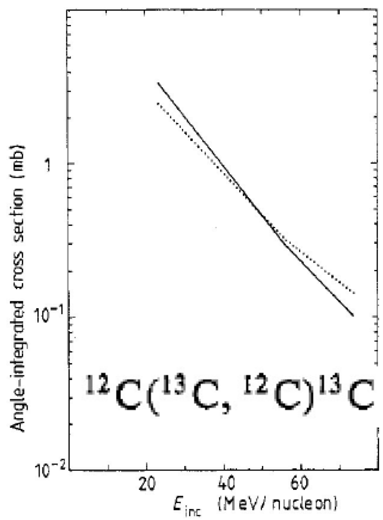

Volume 151B, number 2 PHYSICS LET

TRANSFER OF NUCLEONS AT HIGH RELATIVE VI

W. VON OERTZEN [1]

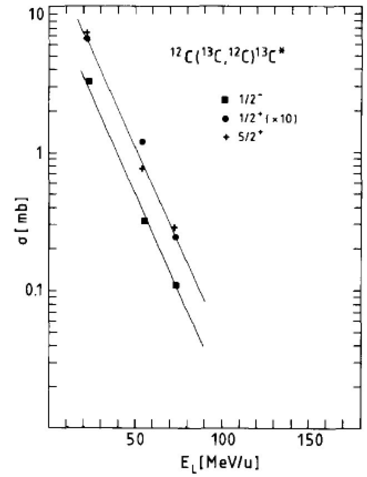

Fig. 3. Total cross section for the transfer of a neutron in the system ^{13}C + ^{12}C leading to different final states of ^{13}C as function of incident energy. The points represent finite range DWBA calculations.

Volume 203, number 4 PHYSICS LETTERS B 7 April 1988

ENERGY DEPENDENCE OF ^{12}C+^{12}C SINGLE-NEUTRON TRANSFER CROSS SECTIONS

J.S. WINFIELD, Sam M. AUSTIN, G.M. CRAWLEY, C. DJALALI [1], C.A. OGILVIE, R.J. SMITH [2], Ziping CHEN and M. TORRES [3]

National Superconducting Cyclotron Laboratory and Department of Physics and Astronomy, Michigan State University, East Lansing, MI 48224-1321, USA

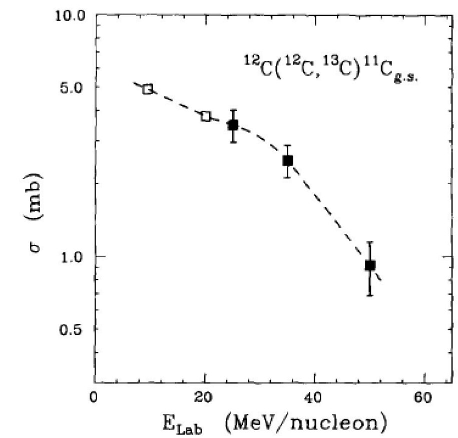

Fig. 3. Dependence of ^{12}C(^{12}C, ^{13}C)^{11}C$_{g.s.}$ angle-integrated cross sections on incident energy. The solid symbols are the present results with systematic error bars indicated. The open symbols are results taken from ref. [14] (20 MeV/nucleon) and ref. [15] (10 MeV/nucleon). The dashed line is to guide the eye.

Angular distributions in high-energy heavy-ion reactions are generally rather featureless and in this paper we concentrate on calculating the **total cross section.**

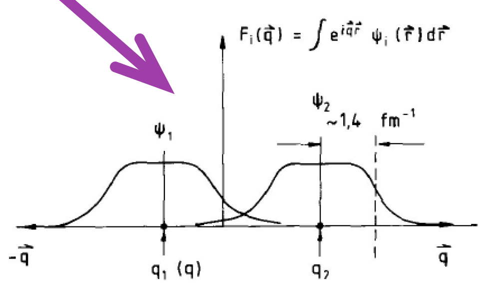

Fig. 2. Schematic representation of the two momentum distributions of the bound state (b + c), ψ_1 and (A + c), ψ_2 separated by the total momentum change $|Q| = |k_f c/B + k_i c/a|$.

INFN Angela Bonaccorso
Istituto Nazionale di Fisica Nucleare
Sezione di Pisa

Puzzle of absolute cross sections solved by semiclassical methods with asymptotic wave functions and energy dependent optical potentials

Problem

- S.C. Pieper et al.,Phys. Rev. Cl8 (1978) 180
- C. Olmer et al., Phys. Rev. Cl8 (1978) 205

Solution

Nuclear Physics **A522** (1991) 578–590
North-Holland

ENERGY DEPENDENCE OF ONE-NUCLEON TRANSFER IN HEAVY-ION COLLISIONS

J.H. SØRENSEN and A. WINTHER

The Niels Bohr Institute, University of Copenhagen, Blegdamsvej 17, DK-2100 Copenhagen Ø, Denmark

G. POLLAROLO

5. Conclusion

It has for some time been a puzzling problem that standard DWBA calculations were not able to reproduce the absolute cross sections for the single-proton stripping reactions for the collision of ^{16}O on ^{208}Pb at all bombarding energies [8–10]) while for the corresponding ^{12}C+^{208}Pb transfer reactions the absolute values were reproduced [11–13]). However, it is the conclusion of the present investigations that taking into account an energy dependence (eq. (2.6)) of the depth of the nuclear part of the interaction U_{1A} together with a consistent use of spectroscopic factors for the individual states at all bombarding energies and for all reactions lead to absolute agreement with the data.

 NP A442 (1985) 381

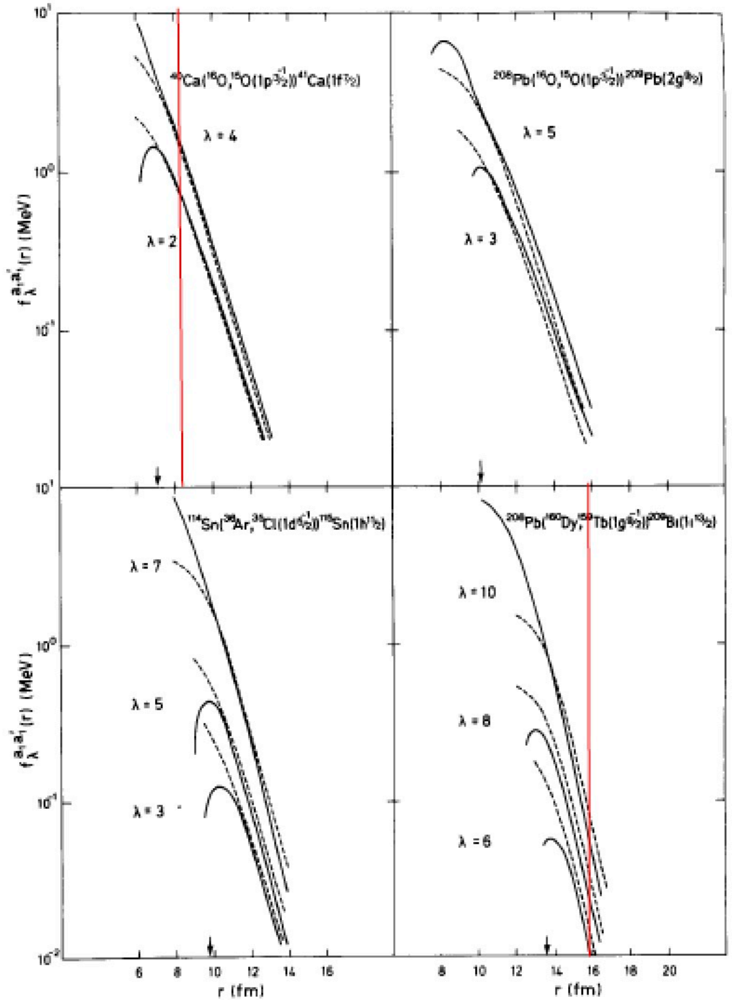

Fig 5 Single-particle form factors calculated making use of eq (30) and figs 1–4 (dashed curves), in comparison with the "exact" form factor given by eq (9) (continuous curves) The arrow on the ordinate indicates the value of the sum of the two radii $R_a + R_A$ where $R_i = 1.2 A^{1/3}$ fm ($i = a, A$) The transfer takes place as a rule at distances larger than $R_a + R_A$

INFN Angela Bonaccorso
Istituto Nazionale di Fisica Nucleare
Sezione di Pisa

Experimental data vs. **Reaction theory** vs. Structure theory

- Direct reactions involve few nucleons and few degrees of freedom but to “model” them requires understanding the whole nucleus and all other possible reactions. Ex: **elastic scattering and the optical potential.**(cf**.** M.Borge talk**)**
- It requires also the understanding of **experimental setups** and the handling of data to extract meaningful observables.
- It has to be **simple and transparent** in its interpretation to help disentangling the physical processes and allow experimentalists to describe their data.
- Reaction theorists must understand **stucture models** (cf. S. Bacca and Shan-Gui Zhou talks) , experiments and they must describe data reliably but in a simple way.

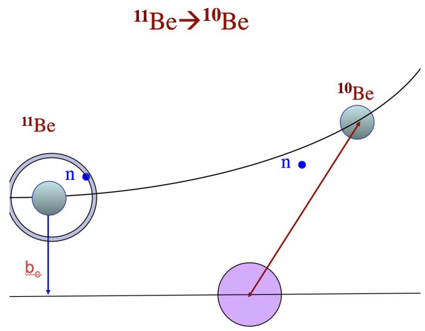

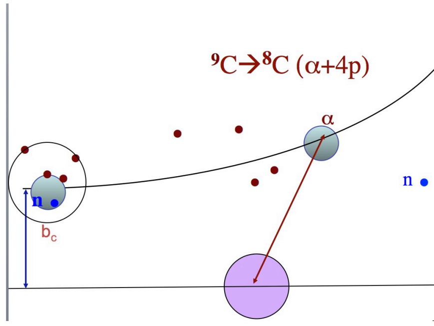

Experimental Setup at SAMURAI at RIBF

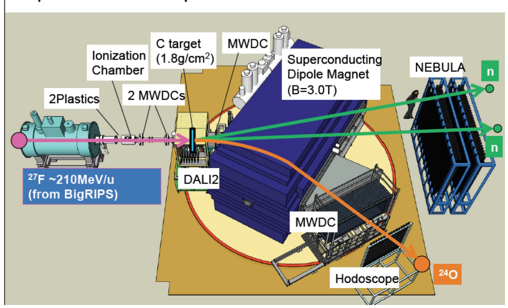

HiRA array

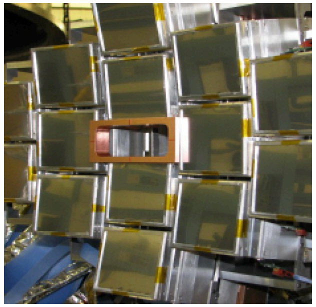

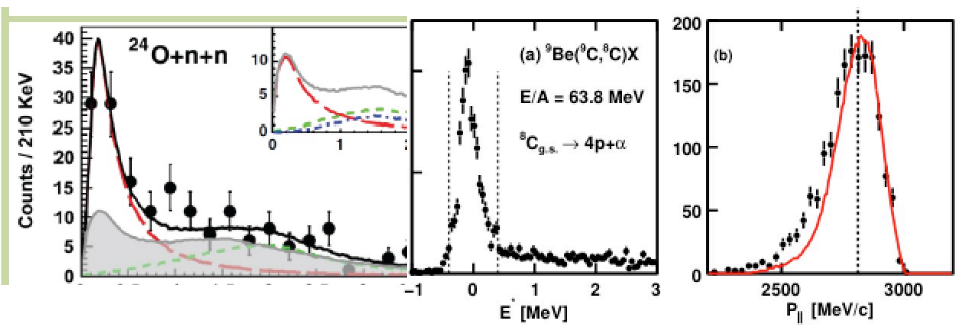

$^{11}Be \rightarrow ^{10}Be$

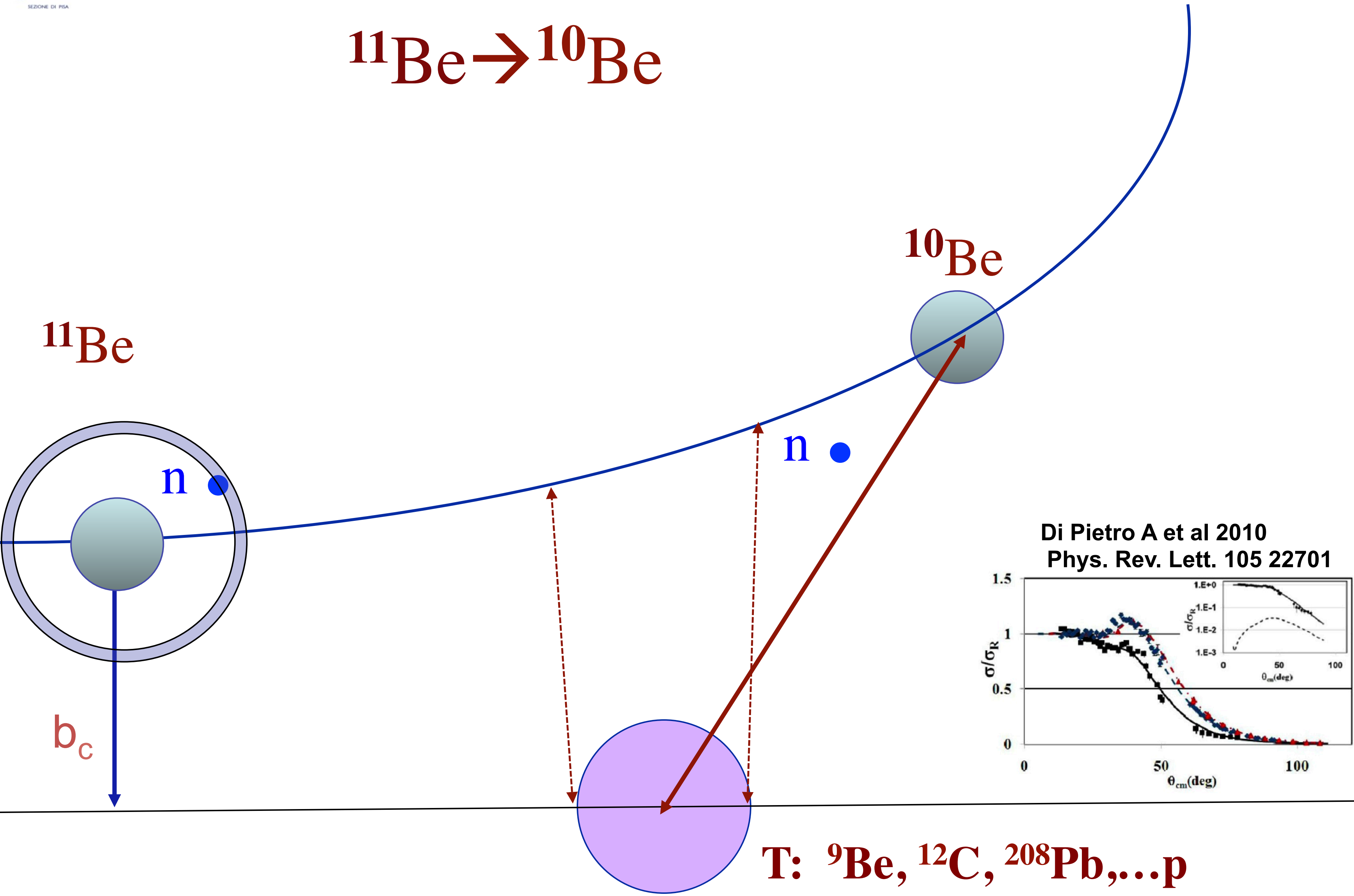

Di Pietro A et al 2010
Phys. Rev. Lett. 105 22701

$^{9}C \rightarrow {}^{8}C\ (\alpha+4p)+n$

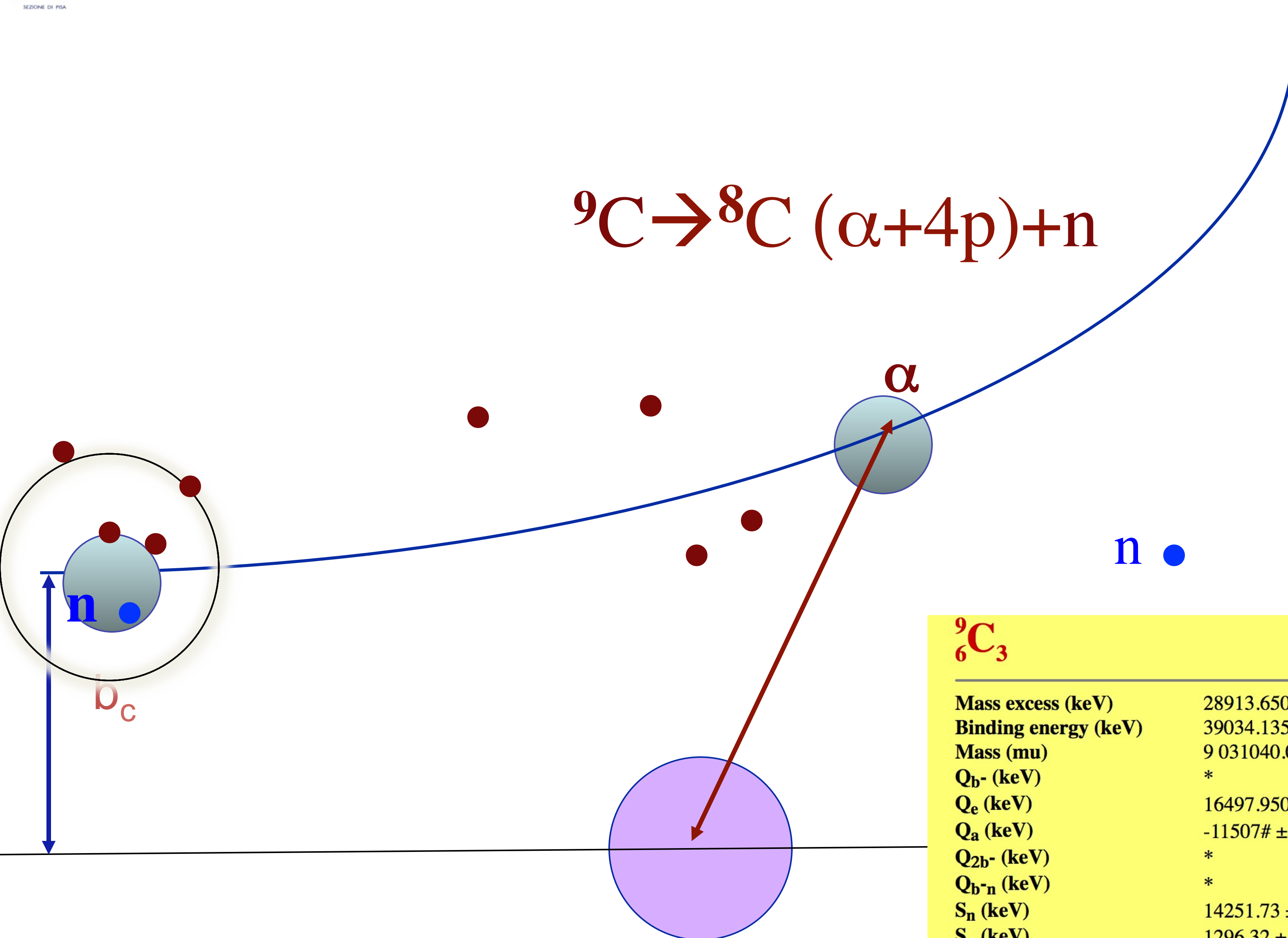

$^{9}_{6}C_{3}$

Mass excess (keV)	28913.650 ± 2.178
Binding energy (keV)	39034.135 ± 2.178
Mass (mu)	9 031040.087 ± 2.338
Q_{b}- (keV)	*
Q_{e} (keV)	16497.950 ± 2.374
Q_{a} (keV)	-11507# ± 3996#
Q_{2b}- (keV)	*
Q_{b}-$_{n}$ (keV)	*
S_{n} (keV)	14251.73 ± 23.17
S_{p} (keV)	1296.32 ± 2.35
S_{2n} (keV)	*
S_{2p} (keV)	1433.78 ± 2.13

INFN Angela Bonaccorso
Istituto Nazionale di Fisica Nucleare

Proton unbound nuclei via invariant mass method

Interest: Two-proton radioactivity vs. 2n-halo by isospin symmetry
^{5}He, ^{6}He, ^{8}He, ^{12}Be and IMME

Isobaric Multiplet Mass Equation

Proton unbound nuclei

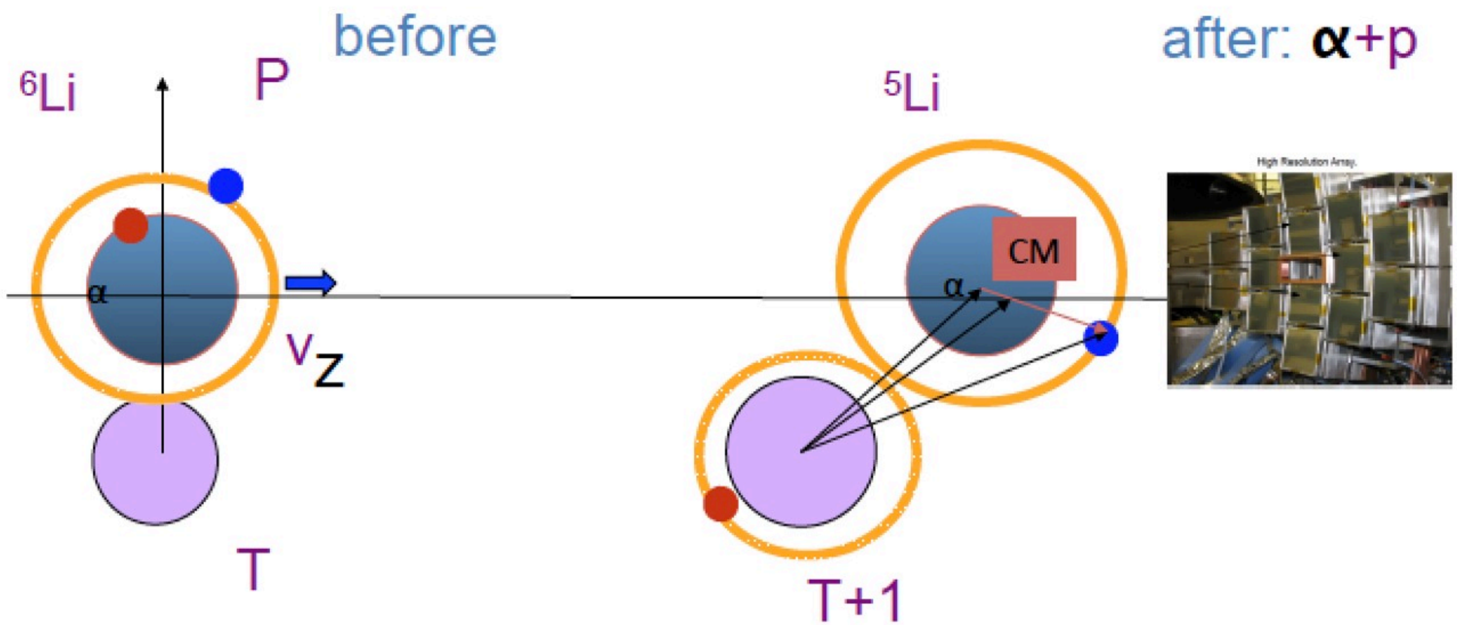

^{6}Li, ^{7}Be, ^{9}C, ^{13}O studied by knockout of a deeply bound **neutron**:

R. J. Charity & HiRA collaboration

Another motivation

p-p chain

$$p(p,\ \beta^+\nu)d(p,\gamma)^3He(\alpha,\gamma)^7Be(p,\gamma)^8B(p,\gamma)^9C(\beta^+\nu)^9B(p)^8Be(\alpha)\alpha.$$

Determine ANC and/or spectroscopic factor for s.p. states
(can give reaction rates directly)
Ab-initio (i.e. Nollett-Wiringa) or HF wfs

NP1412-SAMURAI29R1 (re-evaluation: NP0906-RIBF13)

Title: Inclusive and exclusive breakup of ^{9}C in nuclear and Coulomb fields

Spokesperson: Livius Trache

Approved —Grade A 3 days (including 0.5 days for the BigRIPS tuning)

Collaborators:
F. Carstoiu, RJ Charity
C. Bertulani, T. Motobayashi, L. Sobotka, L. Trache
[Bucharest, St Louis, RIKEN, Texas-Commerce, Pisa]

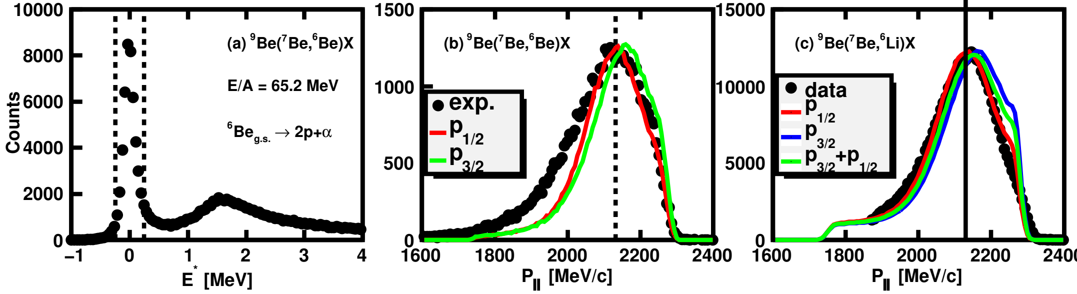

FIGURE 2. (a) Experimental ^{6}Be invariant-mass spectrum and (b,c) the parallel-momentum distributions [3] of the reactions: ^{9}Be(^{7}Be,^{6}Be)X, ^{9}Be(^{7}Be,^{6}Li)X at mid-target energy of 65.2AMeV. Here and the following figures the dashed line on the $P_{||}$ spectra indicates the momentum of the unreacted beam. The dashed lines in (a) show the gate on the ^{6}Be ground state.

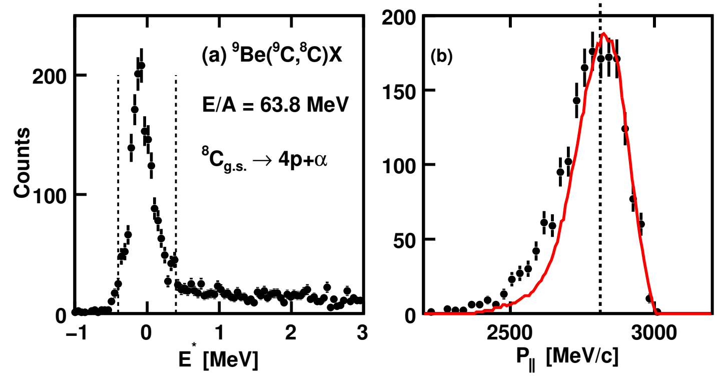

FIGURE 3. (a) The experimental ^{8}C invariant-mass spectrum and (b) the parallel-momentum distributions [3] of the reactions: ^{9}Be(^{9}C,^{8}C)X at mid-target energy of 63.8AMeV. The gate on the ground state of ^{8}C is indicated by the dashed lines in (a)

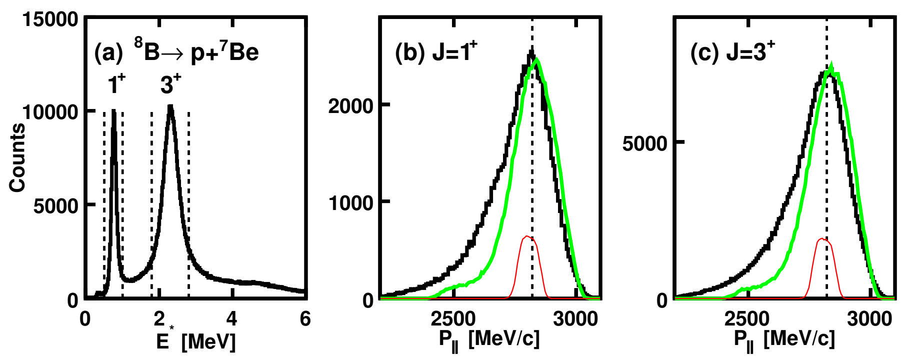

Some of these nuclei are important in the pp-chain, we try to understand their structure from high energy data

RJ Charity et al., private comm.

	E_{inc} AMeV	σ_{exp} mb
$\langle {}^7Be\vert{}^6Be_{g.s}\rangle$	65.2	10
$\langle {}^7Be\vert{}^6Li_{g.s}\rangle$	65.2	50
$\langle {}^9C\vert{}^8C_{g.s}\rangle$	63.8	3.82
$\langle {}^9C\vert{}^8B_{g.s}\rangle$	64.4	54.5
$\langle {}^9C\vert{}^8B_{1+}\rangle$	64.4	12.2
$\langle {}^9C\vert{}^8B_{3+}\rangle$	64.4	42.6

Perfect example of most discussed reaction mechanisms vs. structure topics of present day physics with RIBs

- Unbound nuclei
- n-knockout from deeply bound states
- Reduced cross sections
- Elastic scattering
- Total reaction cross sections

transfer and inelastic excitations

A consistent formalism for all breakup reaction mechanisms

The core-target movement is treated in a semiclassical way, but neutron-target and/or neutron-core with a full QM method.

AB and DM Brink, PRC38, 1776 (1988), PRC43, 299 (1991), PRC44, 1559 (1991).

Early eikonal model: I. Tanihata, Prog. Part. Nucl. Phys. 35, 505 (1995), halo-core decoupling.

$$\frac{d\sigma}{d\xi} = C^2 S \int_0^\infty d\mathbf{b_c} \frac{dP_{-n}(b_c)}{d\xi} P_{ct}(b_c),$$

$\otimes$

$$\xi \to \varepsilon_f, k_z, P_{//} \quad also \quad ANC = \sqrt{C^2 S C_i^2}$$

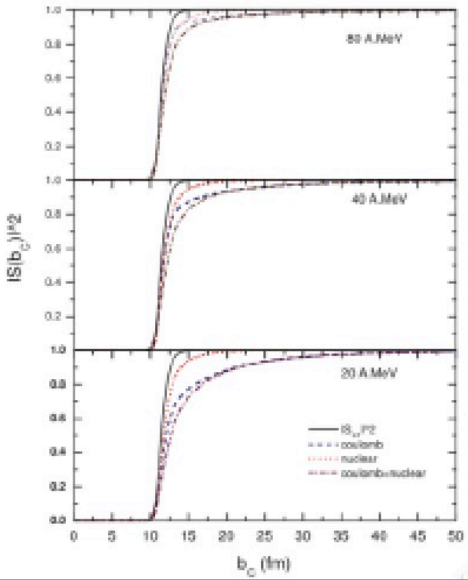

Use of the simple parametrization

$$P_{ct}(b_c) = |S_{ct}|^2 = e^{(-\ln 2 exp[(R_s - b_c)/a])},$$

$$R_s \approx r_s(A_p^{1/3} + A_t^{1/3}) \qquad r_s \approx 1.4fm$$

'strong absorption radius'

AB&F.Carstoiu, NPA706 (2002) 322
AB&A.Ibraheem, NPA748 (2005) 414

Transfer to the continuum: from resonances to knockout reactions

First order time dependent perturbation theory amplitude: **

$$A_{fi} = \frac{1}{i\hbar}\int_{-\infty}^{\infty} dt < \phi_f(\mathbf{r})|V(\mathbf{r})|\phi_i(\mathbf{r}-\mathbf{R}(t)) > e^{-i(\omega t - mvz/\hbar)} \qquad (1)$$

$$\omega = \varepsilon_i - \varepsilon_f + \frac{1}{2}mv^2 \qquad \mathbf{R}(t) = \mathbf{b_c} + vt$$

$$\begin{aligned}\frac{dP_{-n}(b_c)}{d\varepsilon_f} &= \frac{1}{8\pi^3}\frac{m}{\hbar^2 k_f}\frac{1}{2l_i+1}\Sigma_{m_i}|A_{fi}|^2 \\ &\approx \frac{4\pi}{2k_f^2}\Sigma_{j_f}(2j_f+1)(|1-\bar{S}_{j_f}|^2 + 1 - |\bar{S}_{j_f}|^2)\mathcal{F},\end{aligned}$$

ϕ_f see (*)

$$\mathcal{F} = (1 + F_{l_f,l_i,j_f,j_i})B_{l_f,l_i} \qquad B_{l_f,l_i} = \frac{1}{4\pi}\left[\frac{k_f}{mv^2}\right]|C_i|^2\frac{e^{-2\eta b_c}}{2\eta b_c}M_{l_f l_i}$$

Status of the Art
Reaction cross sections of unstable nuclei

Constrain the (nucleus-nucleus) S-matrix $|S|^2$ by total reaction cross section calculations vs exp. data

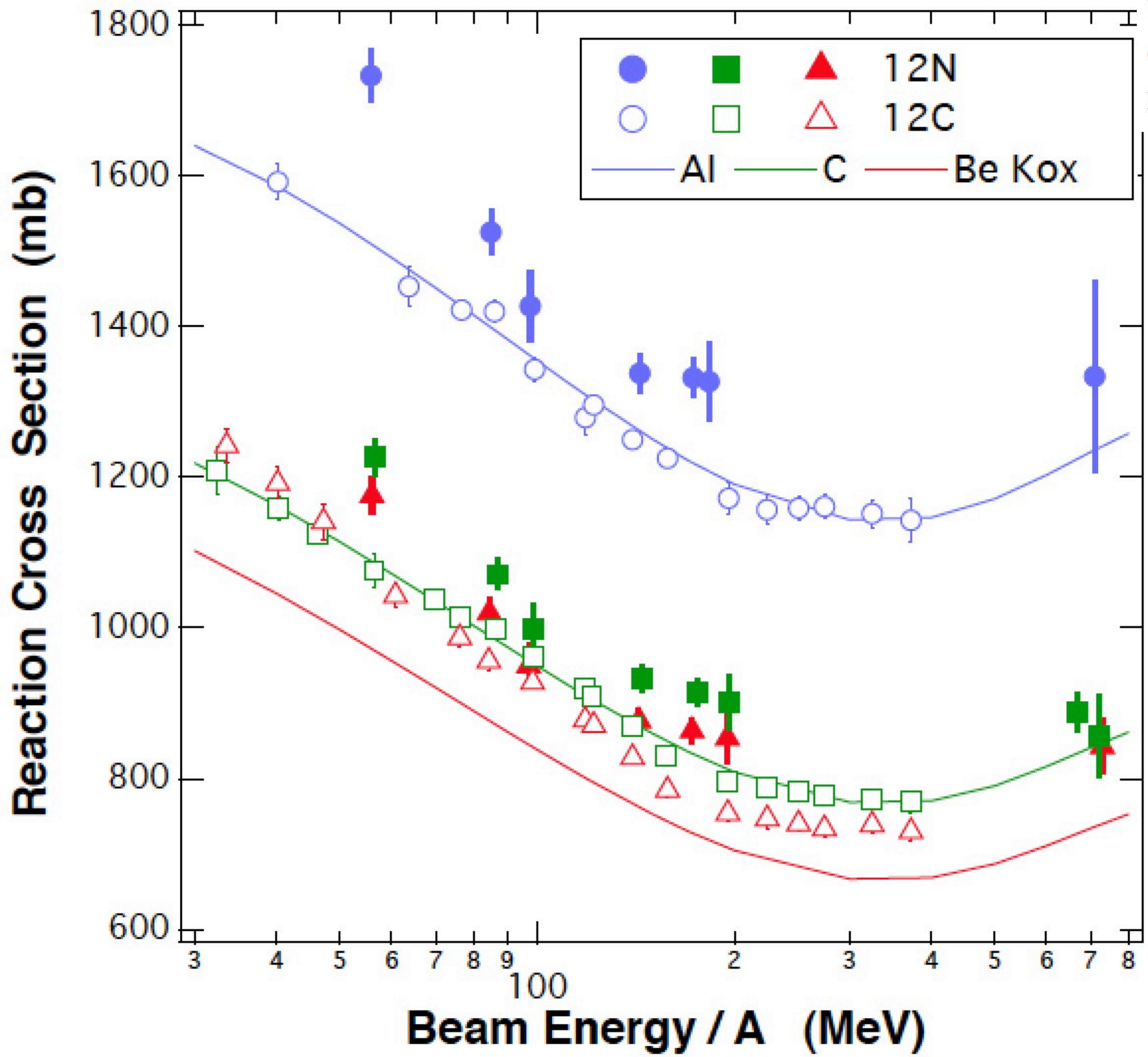

See for example

http://www.sinap.ac.cn/china-japan/

A. Ozawa (University of Tsukuba)

Also

C. Xiangzhou, F. Jun, S.Wenqing, M. Yugang,W. Jiansong, and Y. Wei, Phys. Rev. C58 (1998) 572.

G. W. Fan et al., Phys. Rev. C90 (2014) 044321.

M. Fukuda et al., Nucl. Phys. A656 (1999) 209.

Nuclide	Z	N	S_n (keV)	S_p (keV)
^{12}C	6	6	18721.85 ± 0.95	15956.95 ± 0.42

Nuclide	Z	N	S_n (keV)	S_p (keV)
^{12}N	7	5	15693.76 ± 180.00	601.42 ± 1.38

Proc. Conf. Advances in Radioactive Isotope Science (ARIS2014)
JPS Conf. Proc. **6**, 030103 (2015)
http://dx.doi.org/10.7566/JPSCP.6.030103

Nucleon Density Distribution of the Proton Drip-Line Nucleus ^{12}N Studied via Reaction Cross Sections

Mitsunori Fukuda[1], Yusuke Morita[1], Daiki Nishimura[2], Maya Takechi[3], Kodai Iwamoto[1], Masaru Wakabayashi[1], Yasuto Kamisho[1], Junichi Ohno[1], Masaomi Tanaka[1], Ryosuke Kanbe[1], Shintaro Yamaoka[1], Mototsugu Mihara[1], Kensaku Matsuta[1], Kenta Yoshinaga[2], Ifan Zhu[2], Junpei Khono[4], Sayaka Yamaki[4], Takeshi Suzuki[4], Takayuki Yamaguchi[4], Shinji Suzuki[6], Masayuki Nagashima[3], Kohsuke Abe[3], Keisuke Tashiro[3], Akira Honma[3], Takashi Ohtsubo[3], Takuji Izumikawa[5], Shinji Sato[6], Shigekazu Fukuda[6], and Atsushi Kitagawa[6]

INFN Angela Bonaccorso
Istituto Nazionale di Fisica Nucleare
SEZIONE DI PISA

A target used very often is ^{9}Be → single folding of a n-^{9}Be phenomenological potential with a microscopic projectile density

PHYSICAL REVIEW C **94**, 034604 (2016)

Imaginary part of the ^{9}C-^{9}Be single-folded optical potential

A. Bonaccorso,[1,*] F. Carstoiu,[2] and R. J. Charity[3]

Few-Body Syst (2016) 57:331–336
DOI 10.1007/s00601-016-1082-4

A. Bonaccorso · F. Carstoiu · R. J. Charity · R. Kumar
G. Salvioni

Differences Between a Single- and a Double-Folding Nucleus-^{9}Be Optical Potential

The Glauber reaction cross section is given by

$$\sigma_R = 2\pi \int_0^\infty b\, db(1 - |S_{NN}(\mathbf{b})|^2) \quad (1)$$

where

$$|S_{NN}(\mathbf{b})|^2 = e^{2\chi_I(b)} \quad (2)$$

is the probability that the nucleus-nucleus (NN) scattering is elastic for a given impact parameter **b**.

The imaginary part of the eikonal phase shift is given by

$$\chi_I(\mathbf{b}) = \frac{1}{\hbar v}\int dz\, W^{NN}(\mathbf{b}, z) = \frac{1}{\hbar v}\int dz \int d\mathbf{r_1} W^{nN}(\mathbf{r_1} - \mathbf{r})\rho(\mathbf{r_1}) \quad (3)$$

where W^{NN} is negative defined as

$$W^{NN}(\mathbf{r}) = \int d\mathbf{b_1} W^{nN}(\mathbf{b_1} - \mathbf{b}, z) \int dz_1\, \rho(\mathbf{b_1}, z_1). \quad (4)$$

In the double-folding method, W^{NN} is obtained from the microscopic densities $\rho_{p,t}(\mathbf{r})$ for the projectile and target respectively and an energy-dependent nucleon-nucleon (nn) cross section σ_{nn}, i.e.,

$$W^{NN}(\mathbf{r}) = -\frac{1}{2}\hbar v \sigma_{nn} \int d\mathbf{b_1}\, \rho_p(\mathbf{b_1} - \mathbf{b}, z) \int dz_1\, \rho_t(\mathbf{b_1}, z_1). \quad (5)$$

Also

$$W^{nN}(\mathbf{r}) = -\frac{1}{2}\hbar v \sigma_{nn} \rho_t(\mathbf{r}) \quad (6)$$

is a single-folded zero-range n-target imaginary potential and v is the nucleon-target velocity of relative motion. The W^{nN} potential of Eq.(6) has the same range as the target density because σ_{nn} is a simple scaling factor.

A.B & R. J. Charity, PRC89, 024619 (2014)

Resonances described by $\delta V(r) = 16\alpha \frac{e^{2(r-R^R)/a^R}}{(1+e^{(r-R^R)/a^R})^4}$. consistent with dispersive contribution

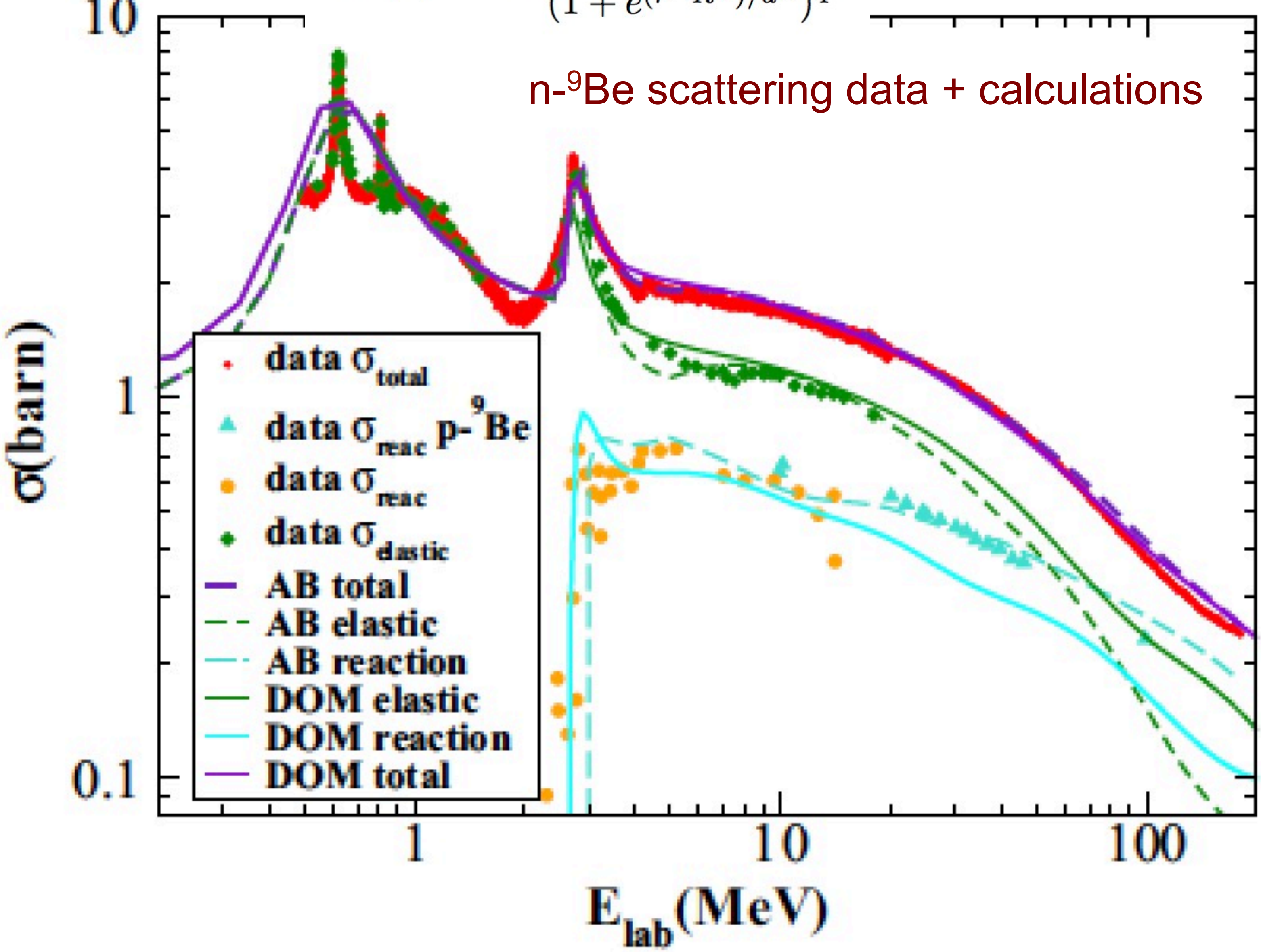

Angela Bonaccorso
Istituto Nazionale di Fisica Nucleare

n+^{9}Be

…. SF VMC density & σ_{np} & σ_{pp}- parametrized according to C. A. Bertulani, and C. De Conti, Phys. Rev. C81 (2010) 064603.
AB phenomenological, DOM

65 MeV

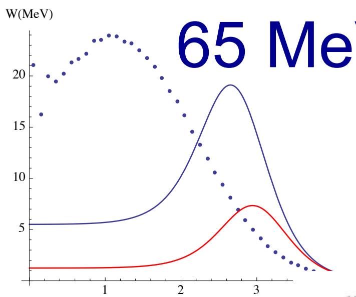

40 MeV

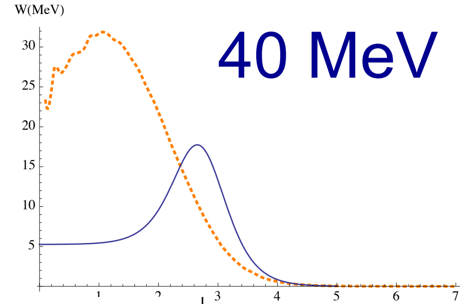

^{9}C+^{9}Be

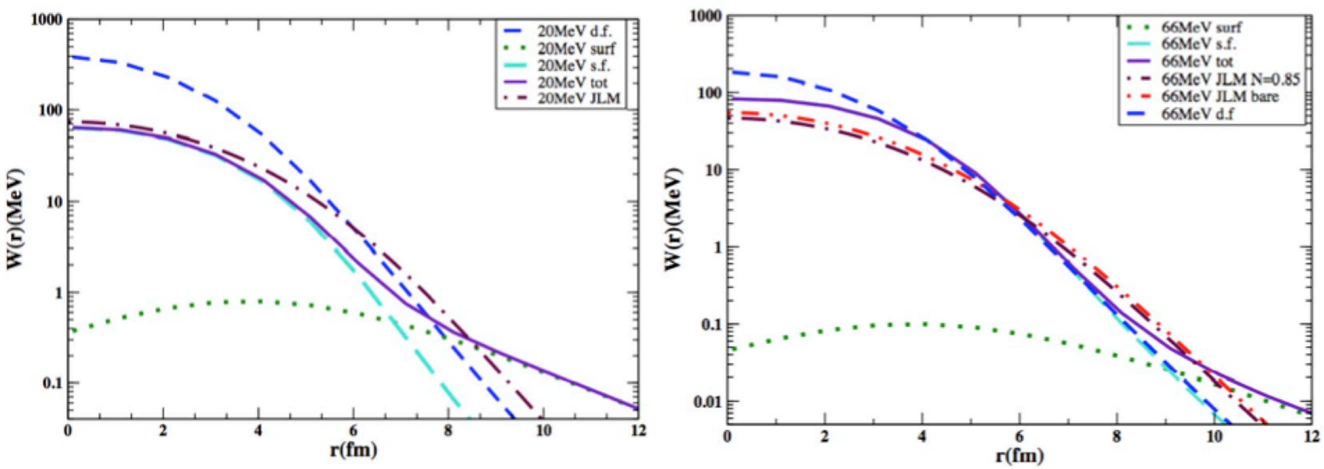

E_{lab} (A.MeV)	$J_{d.f.HF}$ (MeV fm^3)	rms (fm)	J^{ren}_{JLM} (MeV fm^3)	rms (fm)	$J^{+surf}_{s.fold}$ (MeV fm^3)	rms (fm)	$J_{s.fold}$ (MeV)	rms	W_{surf}
20	656	3.55	259	4.42	198	4.72	172	3.81	0.8
38	437	3.55	212	4.40	272	4.29	255	3.85	0.5
66	301	3.55	143	4.31	248	3.96	245	3.86	0.1
83	261	3.55	147	4.27	232.2	3.87	231.7	3.85	0.015

$$W(r) = -4a^i W_{surf}\frac{d}{dr}\frac{1}{1+e^{(r-R^i)/a^i}}. \qquad (9)$$

with very small strength (W_{surf} =0.8 to 0.015 MeV), the radius has been taken as R^i=3.8 fm, while the diffuseness has been taken large, according to [1; 4], and equal to $a^i = 1/(2\sqrt{2mS_p/\hbar}) = 2$ fm for ^{9}C, since S_p=1.3 MeV.

A. B, and F. Carstoiu, Nucl. Phys. A **706**, 322 (2002).

Advantages with respect to double folding models:

- The imaginary potential is correctly second order because of the phenomenological nature of the n-T potential.
- The projectile density can be better tested because one is free from the ambiguity on the target density.
- The ambiguity on the nucleon-nucleon interaction to be used is overcome.
- The energy dependence of the potential is correctly reproduced because of the underlying correctness of the n-T potential.
- Deformation and surface effects of the target are correctly taken into account and one is left with the task of modelling the same effects for the exotic projectile.

INFN Angela Bonaccorso
Istituto Nazionale di Fisica Nucleare

8Li and 8B data from

8. G. W. Fan et al., Phys. Rev. C90 (2014) 044321.
9. M. Fukuda et al., Nucl. Phys. A656 (1999) 209.

9C data from Fukuda, Nishimura, private communication

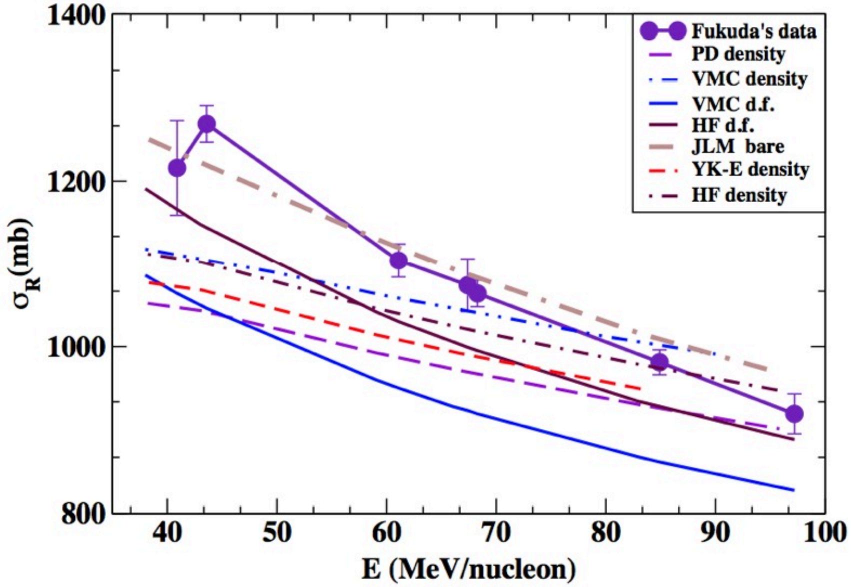

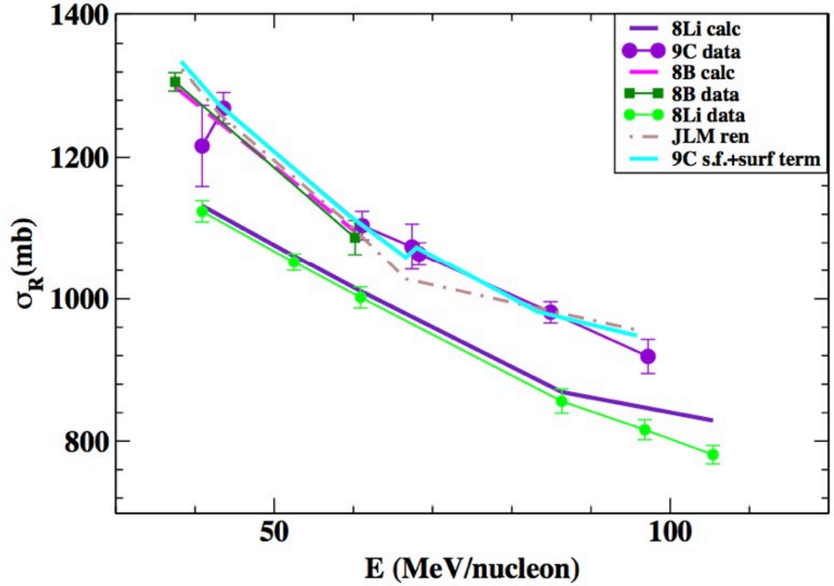

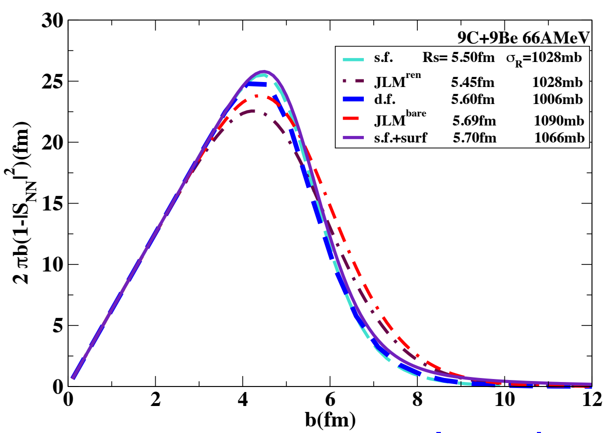

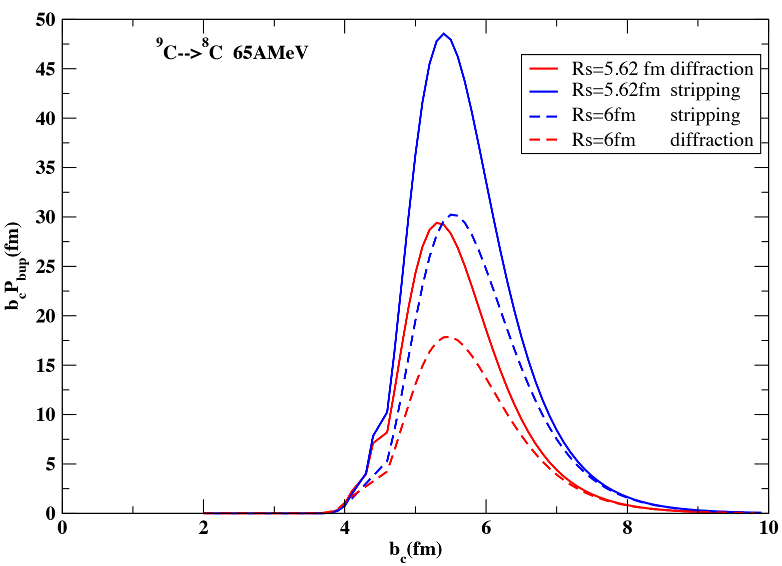

In σ_R large distances are important while breakup is localized around → R_S

INFN Angela Bonaccorso
Istituto Nazionale di Fisica Nucleare

Knockout beyond the dripline
A. Bonaccorso, R. J. Charity, R. Kumar, and G. Salvioni
AIP Conference Proceedings 1645, 30 (2015); doi: 10.1063/1.4909557

TABLE 2. Reaction parameters for the indicated overlaps and cross sections for the corresponding knockout reactions.

	E_{inc} AMeV	σ_{exp} mb	σ_{-n} mb	σ_{-p} mb	$\sigma_{-n_{nop}}$ mb	R_s fm
$\langle ^7Be \vert ^6Be_{g.s} \rangle$	65.2	10	(44.7) 68.24		(10.8) 11.12	(6.0) 5.06
$\langle ^7Be \vert ^6Li_{g.s} \rangle$	65.2	50		54.4		5.2
$\langle ^9C \vert ^8C_{g.s} \rangle$	63.8	3.82	56		(3.86) 42.3 **15**	(6.7) 5.46 **6**
$\langle ^9C \vert ^8B_{g.s} \rangle$	64.4	54.5		46		5.3
$\langle ^9C \vert ^8B_{1+} \rangle$	64.4	12.2		8.73		5.3
$\langle ^9C \vert ^8B_{3+} \rangle$	64.4	42.6		42.3		(5.45)

$r_s = 1.44 \rightarrow R_s = 6.00\text{fm} \rightarrow \sigma_R = 15$ mb

1.35	5.62	22.8
1.31	5.46	42.3

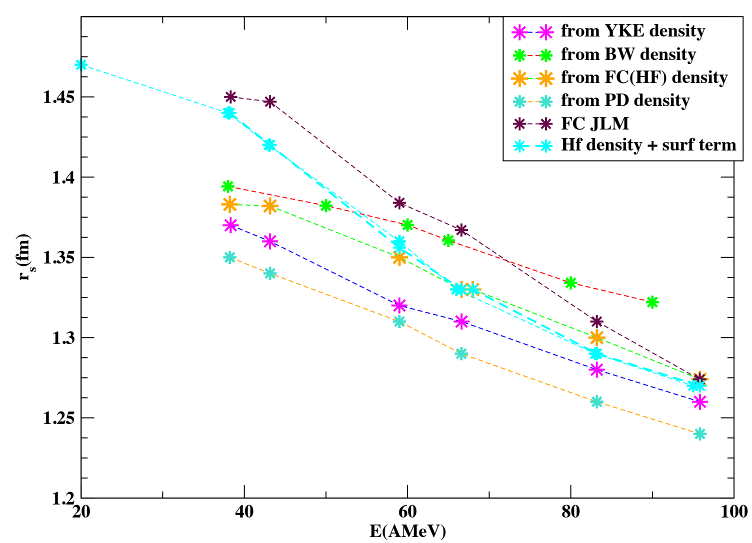

INFN Angela Bonaccorso
Istituto Nazionale di Fisica Nucleare

N-Z Asymmetry dependence of spectroscopic factors

PHYSICAL REVIEW C 76, 044314 (2007)

Dispersive-optical-model analysis of the asymmetry dependence of correlations in Ca isotopes

R. J. Charity,[1] J. M. Mueller,[2] L. G. Sobotka,[1,2] and W. H. Dickhoff[2]

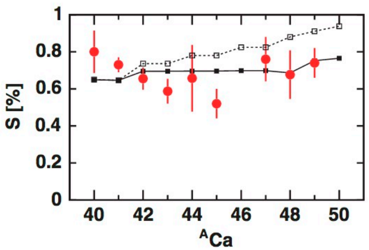

FIG. 14. (Color online) Data points indicate spectroscopic factors deduced by Lee *et al.* [75] for valance neutron hole and particle states in Ca isotopes using (p, d) and (d, p) reactions. The spectroscopic factors are expressed as a percent of the independent-particle-model value. The DOM predictions with the asymmetry dependences D_1 [see Eq. (32)] and D_2 [Eq. (39)] are indicated by the points connected with dashed and solid lines, respectively.

Neutron-Proton Asymmetry Dependence of Spectroscopic Factors in Ar Isotopes

Jenny Lee (李曉菁),[1] M. B. Tsang (曾敏兒),[1] D. Bazin,[1] D. Coupland,[1] V. Henzl,[1] D. Henzlova,[1] M. Kilburn,[1] W. G. Lynch (連致標),[1] A. M. Rogers,[1] A. Sanetullaev,[1] A. Signoracci,[1] Z. Y. Sun (孙志宇),[1,2] M. Youngs,[1] K. Y. Chae,[3] R. J. Charity,[4] H. K. Cheung (張凱傑),[5] M. Famiano,[6] S. Hudan,[7] P. O'Malley,[8] W. A. Peters,[8] K. Schmitt,[3] D. Shapira,[9] and L. G. Sobotka[4]

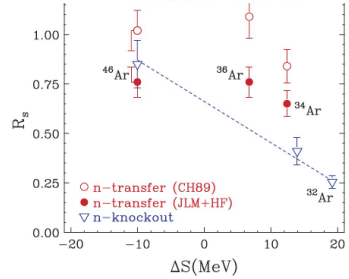

FIG. 2 (color online). Reduction factors Rs = SF(expt)/SF(LB-SM) as a function of the difference between neutron and proton separation energies, ΔS. The solid and open circles represent Rs deduced in JLM + HF and CH89 approach using the present transfer reaction data, respectively. The open triangles denote the Rs from knockout reactions [11]. The dashed line is the best fit of Rs of ^{32,34,46}Ar from knockout reactions. The use of different ΔS values from the present work and knockout reactions in Ref. [11] is explained in Ref. [28].

Quenching of Cross Sections in Nucleon Transfer Reactions

B. P. Kay,[1,2,*] J. P. Schiffer,[1] and S. J. Freeman[3]

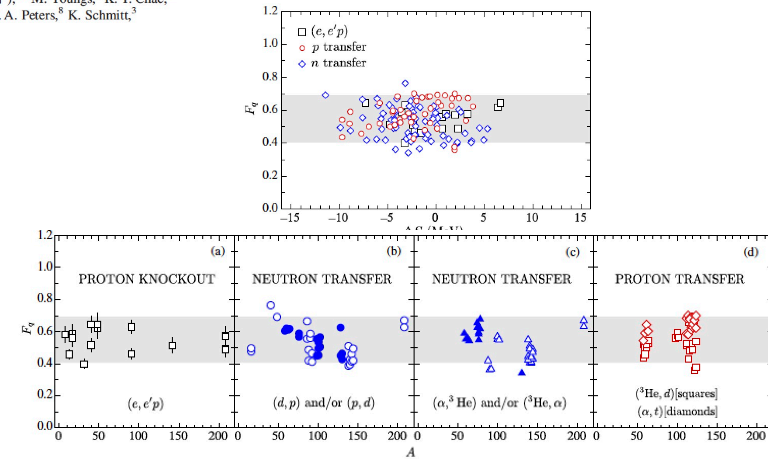

FIG. 1 (color online). The quenching factor F_q versus target mass A. The $(e, e'p)$ data in panel (a) are from Refs. [7,35]. The band represents the mean $\pm 2\sigma$ of the $(e, e'p)$ data to guide the eye. The data in panels (b), (c), (d) are from this analysis and tabulated in the Supplemental Material [26]. Solid symbols are from adding and removing reactions while the empty ones are from adding or just removing.

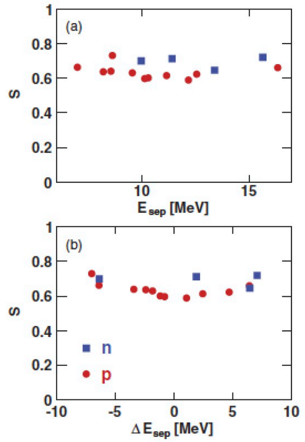

FIG. 27. (Color online) Spectroscopic factors (relative to the independent-particle-model value) for valence-hole levels determined from the fitted potentials. Results are shown for the $Z = 20$, 28 and $N = 28$ and circular points represent neutrons and protons, respectively. In (a), these are plotted versus the separation energy of the level, while in (b), they are plotted versus the difference in proton and neutron separation energies.

122503 (2013) PHYSICAL REVIEW LETTERS week ending 22 MARCH 2013

Limited Asymmetry Dependence of Correlations from Single Nucleon Transfer

...y,[1,2] A. Gillibert,[1] L. Nalpas,[1] A. Obertelli,[1] N. Keeley,[3] C. Barbieri,[4] D. Beaumel,[5] S. Boissinot,[1] G. Burgunder,[6] ...lone,[4,7,8] A. Corsi,[1] J. Gibelin,[9] S. Giron,[5] J. Guillot,[5] F. Hammache,[5] V. Lapoux,[1] A. Matta,[5] E. C. Pollacco,[1] R. Raabe,[6,2] M. Rejmund,[6] N. de Séréville,[5] A. Shrivastava,[6] A. Signoracci,[1] and Y. Utsuno[10]

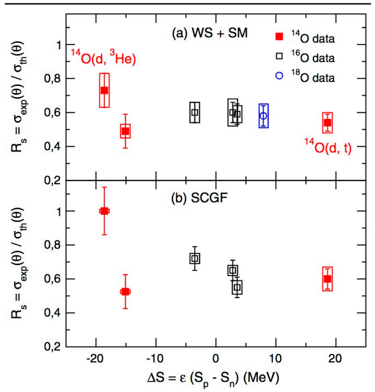

FIG. 4 (color online). Reduction factors R_s obtained with (a) a WS OF and the SLy4 averaged over four entrance and two exit potentials, and compared to shell-model calculations performed with the WBT interaction [37] in the $0p + 2\hbar\omega$ valence space; (b) a microscopic (SCGF) form factor [30]. The detail of error bars is given in text.

PHYSICAL REVIEW C 83, 064605 (2011)

Asymmetry dependence of nucleon correlations in spherical nuclei extracted from a dispersive-optical-model analysis

J. M. Mueller,[1,*] R. J. Charity,[2] R. Shane,[1] L. G. Sobotka,[1,2] S. J. Waldecker,[1] W. H. Dickhoff,[1] A. S. Crowell,[3] J. H. Esterline,[3] B. Fallin,[3] C. R. Howell,[3] C. Westerfeldt,[3] M. Youngs,[4] B. J. Crowe III,[5] and R. S. Pedroni[6]

Reduction Factors from (p,2p) Cross Sections for $^{14-23}$O Projectiles

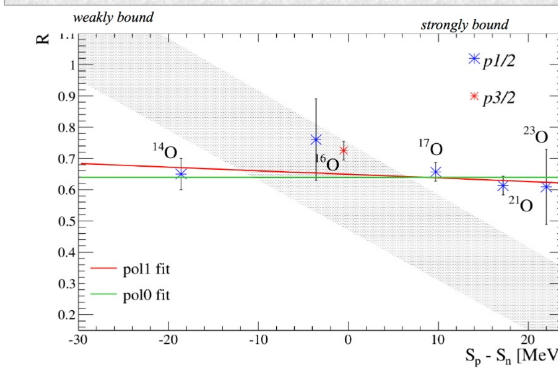

Reduction factor
$R = \sigma_{exp}/\sigma_{theo(IPM)}$

- A weak or no dependence of single-particle strength on the isospin asymmetry
- In contrast to the observed trend from knockout reactions at intermediate energies using composite targets
- Comparable with the ab-initio Green's function and coupled cluster calculations as well as (e,e'p) data

L. Atar, Panin, Paschalis, Aumann, Bertulani et al. for the R3B collaboration

INFN Angela Bonaccorso

Unbound Nuclei "levels"

Available online at www.sciencedirect.com
ScienceDirect
Nuclear Physics A 791 (2007) 303–312

^{10}Li spectrum from ^{11}Li fragmentation

G. Blanchon [a], A. Bonaccorso [a,*], D.M. Brink [b], N. Vinh Mau [c]

Table 3
Scattering length of the 2s continuum state, energies and widths of the p- and d-resonances in ^{10}Li and corresponding strength parameters for the δV potential

	ε_{res} (MeV)	Γ_j (MeV)	a_s (fm^{-1})	α (MeV)
$2s_{1/2}$			−17.2	−10.0
$1p_{1/2}$	0.63	0.35		3.3
$1d_{5/2}$	1.55	0.18		−9.8

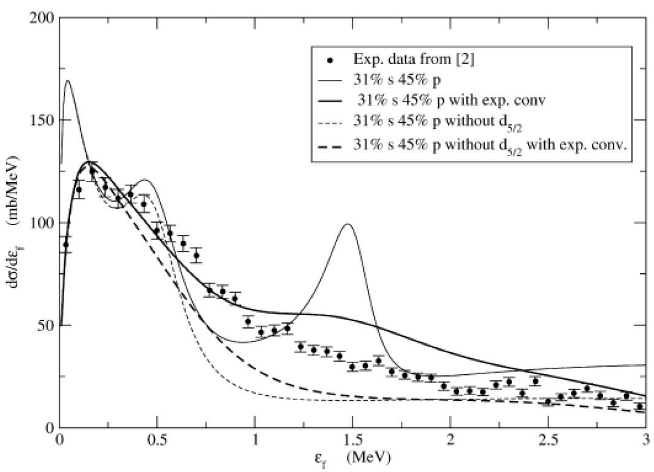

Fig. 2. n–^{9}Li relative energy spectrum, for the reaction $^{11}\mathrm{Li} + {}^{12}\mathrm{C} \to n + {}^{9}\mathrm{Li} + \mathrm{X}$ at 264 A MeV. Only the contributions from an s and p initial state with experimental spectroscopic factors [4] $C^2S = 0.31$ and 0.45 respectively are included. The thin solid curve is the total calculated result. The thick solid curve is after convolution with the experimental resolution function. The thin dashed curve is the calculation without the d-resonance while the thick dashed curve is the same calculation after convolution. The symbols with error bars are the experimental points from [2]. Calculations are normalised to the data.

H. Simon et al., NPA791, 267 (2007)

Physics Letters B 755 (2016) 481–485
Contents lists available at ScienceDirect
Physics Letters B
www.elsevier.com/locate/physletb

Investigation of the role of ^{10}Li resonances in the halo structure of ^{11}Li through the ^{11}Li(p, d)^{10}Li transfer reaction

A. Sanetullaev [a,b,1], R. Kanungo [a,*], J. Tanaka [c], M. Alcorta [b], C. Andreoiu [d], P. Bender [b], A.A. Chen [e], G. Christian [b], B. Davids [b], J. Fallis [b], J.P. Fortin [a,f], N. Galinski [b], A.T. Gallant [b], P.E. Garrett [g], G. Hackman [b], B. Hadinia [g], S. Ishimoto [h], M. Keefe [a], R. Krücken [b,i], J. Lighthall [b], E. McNeice [e], D. Miller [b], J. Purcell [a], J.S. Randhawa [a], T. Roger [j], A. Rojas [b], H. Savajols [j], A. Shotter [k], I. Tanihata [c,l], I.J. Thompson [m], C. Unsworth [b], P. Voss [d], Z. Wang [b,d]

The resonance energy spectrum (Fig. 2b) of ^{10}Li is constructed in the missing mass technique using the measured energy and scattering angle of the deuterons. A very prominent resonance peak is seen at $E_r = 0.62 \pm 0.04$ MeV and full width $\Gamma = 0.33 \pm 0.07$ MeV is obtained from fitting the spectrum with a Voigt function with an energy dependent Breit–Wigner function width [22].

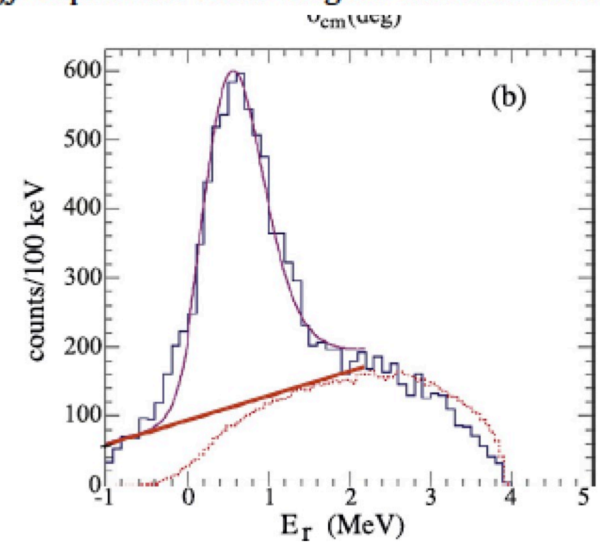

Flagships are still flagship!!!!

(Uesaka san)

State-of-the-art (recent progress)

Traditional methods

- Renewed interest in higly numerical DWBA and CDCC calculations of various aspects of breakup: A. Moro & Co., B.V. Carlson et al., K.Ogata et al.
  So far mainly d-induced reactions.
- Resonant scattering and R-matrix: P. Descouvemont. G. Rogachev
- Various eikonal approaches: best recent results (p,pN): Bertulani-Aumann for R3B collaboration.
- Semiclassical and few body (Hussein, Canto &Co), P. Capel
- Reaction cross sections OK with eikonal approach (Ogawa): improved folding models for the optical potential (Furumoto opt pot)

New methods:

- Chiral interactions used for: ab initio no-core shell model with continuum, and its applications to nucleon and deuterium scattering on light nuclei: P. Navratil, S. Quaglioni, G. Hupin, J. Dohet-Eraly
- Optical potential microscopic calculations from chiral interactions

ECT* workshop

Towards consistent approaches for nuclear structure and reactions
06 Jun 2016 to 10 Jun 2016
Poster Program
Organizers
Carlos Bertulani (Texas A&M University-Commerce) carlos.bertulani@tamuc.edu
Guillaume Blanchon (CEA - DAM - DIF) guillaume.blanchon@cea.fr
Gregory Potel (Lawrence Livermore National Laboratory) potel@nscl.msu.edu
Vittorio Soma (CEA Saclay) vittorio.soma@cea.fr

Open questions:

- Unbound nuclei via projectile fragmentation. SEMICLASSICAL OK, but numerical (DWBA-like still in progress)
- Tetraneutron

Physics beyond the limits of stability: exploring the continuum
17 Oct 2016 to 21 Oct 2016

Organizers
Angela Bonaccorso (INFN Pisa) angela.bonaccorso@pi.infn.it
Nigel Orr (LPC Caen) orr@lpccaen.in2p3.fr

INFN Angela Bonaccorso
Istituto Nazionale di Fisica Nucleare
SEZIONE DI PISA

Nuclei are not anymore what they used to be . . . Re-write Nuclear Physics Textbooks !!

- $R=1.4\text{-}1.5\,(A_p^{1/3}+A_t^{1/3})$fm…….radius

- NN Optical potentials (imag. part) describing elastic scattering and/or reaction cross sections must contain a surface term with very large diffusness 2-3fm.

- nN optical potentials (real part) must contain a term representing particle-vibration couplings or surface oscillations/deformations, consistent with a dispersive contribution **DOM**

$$\delta V(r) = 16\alpha \frac{e^{2(r-R^R)/a^R}}{(1+e^{(r-R^R)/a^R})^4}.$$

"shape"

- Bound&continuum

- Energy dependence ? http://pdg.lbl.gov/2015/reviews/rpp2015-rev-cross-section-plots.pdf

50. Plots of cross sections and related quantities 11

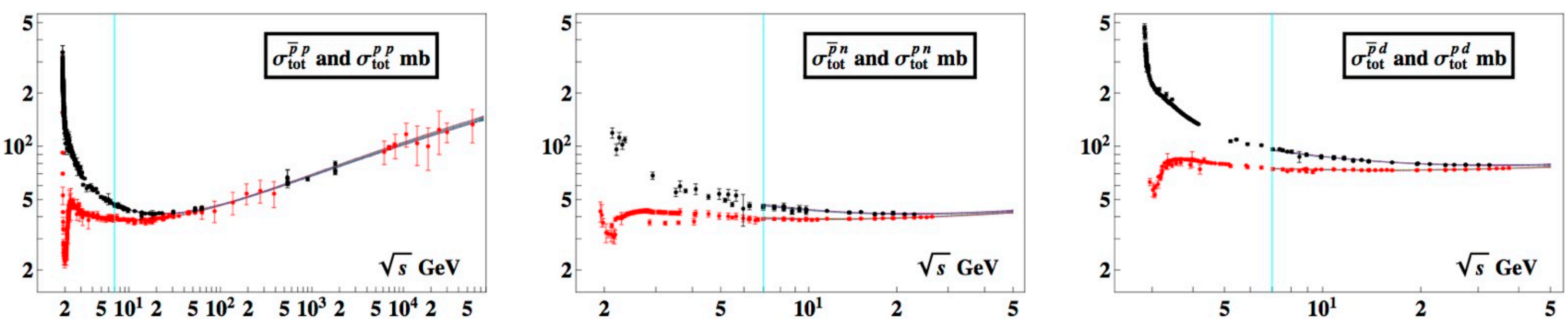

Angela Bonaccorso
Istituto Nazionale di Fisica Nucleare
SEZIONE DI PISA

Outlook

Direct reactions seem to be “quantized” in time over ~30y ranges.

What next for 2017-2050?

- Understanding at a microscopic level the **energy dependence** of nn and NN interactions, including optical potentials.
- **Surface effects, clustering** and **unbound structures** → Will we study mainly unbound nuclei via resonance definition, similarly to particle physics? (cf. W. Nazarewicz).
- Structure and reaction models will be unified via ab-initio methods and full inclusion of continuum spectra (cf S. Bacca, see also **D**ispersive **O**ptical **M**odel).

- Will improvements in numerical techniques allow to solve the nuclear many body problem “exactly”?

and/or

Will semiclassical-analytical methods survive.

INFN Angela Bonaccorso
Istituto Nazionale di Fisica Nucleare
SEZIONE DI PISA

Legenda and thanks to:

M. Fukuda et al., and the R3B collaboration for allowing me to show their results

DOM **Bob Charity**
FC Florin Carstoiu
PD Pierre Descouvemont
Y K-E Yoshiko Kanada-Enyo
ST Stefan Typel
BW Bob Wiringa http://www.phy.anl.gov/theory/research/density/

for providing unpublished data and calculations.

Some more historical collaborators:

David Brink, Nicole Vinh Mau, Guillaume Blanchon, Cristina Rea Ravinder Kumar, the MAGNEX group at LNS-INFN, Catania.

“If you have heart you will certainly have brain…”
(paraphrased from Julian Fellowes)

Courtesy of R J Charity : Egret at dawn in Beachmere Australia

PHYSICAL REVIEW C **90**, 064621 (2014)

First application of the n-^{9}Be optical potential to the study of the ^{10}Be continuum via the (^{18}O, ^{17}O) neutron-transfer reaction

D. Carbone,[1,*] M. Bondì,[1,2] A. Bonaccorso,[3] C. Agodi,[1] F. Cappuzzello,[1,2] M. Cavallaro,[1] R. J. Charity,[4] A. Cunsolo,[1] M. De Napoli,[5] and A. Foti[2,5]

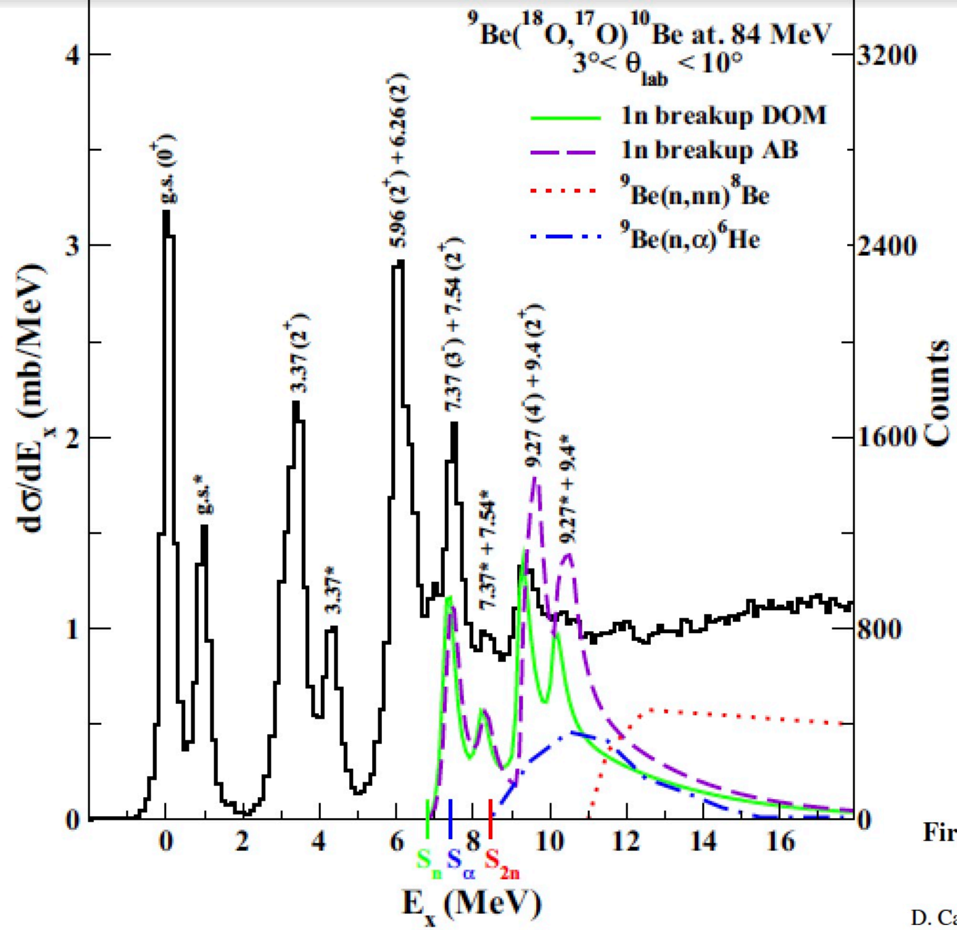

FIG. 2. (Color online) Inclusive excitation energy spectrum of the ^{9}Be(^{18}O, ^{17}O)^{10}Be reaction at 84-MeV incident energy and $3^\circ < \theta_{\rm lab} < 10^\circ$. The background that comes from ^{12}C and ^{16}O impurities has been subtracted. Peaks marked with an asterisk refer to the ^{17}O ejectile emitted in its first excited state at 0.87 MeV. Total $1-n$ breakup calculations that result from the use of the DOM and the AB potentials (see text) [12] are shown as the green-continuous and the violet-dashed lines, respectively. The experimental data [22] of the ^{9}Be(n,nn)^{8}Be [23] and ^{9}Be(n,α)^{6}He [24] reactions are reported as the red-dotted and blue-dotted-dashed lines, respectively. The $1n$-(S_n), $2n$-(S_{2n}), and α-(S_α) separation energies are also indicated.

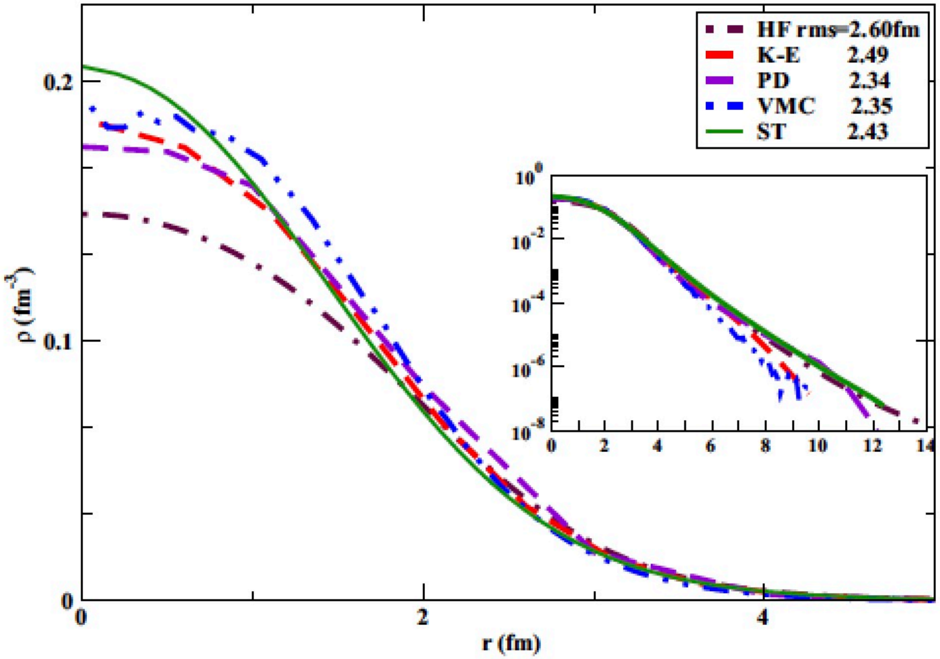

FIG. 4. ^{9}C densities used in the calculated cross sections shown in Fig. 2.

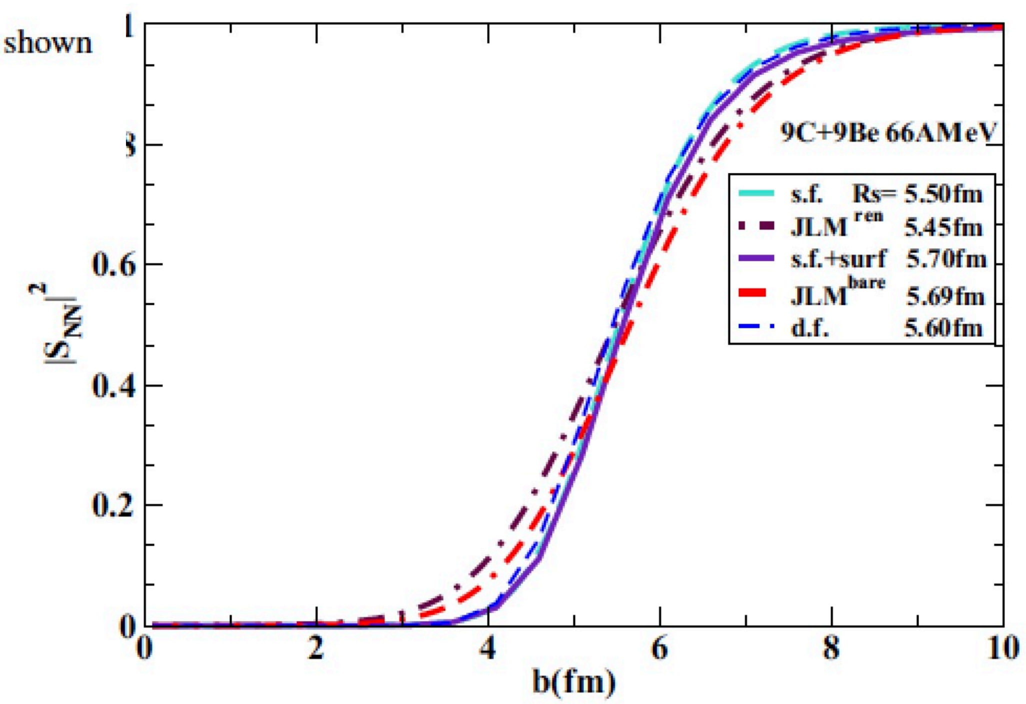

TABLE II. Experimental reaction cross sections, second column, from Ref. [32]. Calculated total reaction cross sections with the double-folded potential using VMC densities for both ^{9}C and ^{9}Be (third column); double-folded potential using HF densities for both ^{9}C and ^{9}Be (fourth column); using the single-folded potential with HF density for ^{9}C (fifth column) and with the added surface potential (sixth column), with the "bare" JLM and with the renormalized JLM for $^9\text{C}+{}^9\text{Be}$. The renormalization factor for the JLM potential and strength of the additional surface potential for the single-folded potential are also given. For the case of $\sigma^{+\text{surf}}_{\text{s.fold}}$ we then give strong-absorption radius R_s from $|S_{NN}(R_s)|^2 = \frac{1}{2}$, and R_S^{fit} from the fit to the calculated $|S_{NN}|^2$ according to Eq. (10). In this case also the diffuseness-like parameter is given. Last column: r_s from Eq. (11) and R_s.

E_{lab} (MeV/nucleon)	σ_{exp} (mb)	$\sigma^{\text{VMC}}_{\text{d.fold}}$ (mb)	$\sigma^{\text{HF}}_{\text{d.fold}}$ (mb)	$\sigma_{\text{s.fold}}$ (mb)	$\sigma^{+\text{surf}}_{\text{s.fold}}$ (mb)	$\sigma^{\text{bare}}_{\text{JLM}}$ (mb)	$\sigma^{\text{ren}}_{\text{JLM}}$ (mb)	N_{JLM}	W_{surf} (MeV)	R_s (fm)	R_s^{fit} (fm)	a^{fit} (fm)	r_s (fm)
20		1267	1409	1078	1565	1338	1538	1.65	0.8	6.12	6.25	1.01	1.47
38		1086	1191	1112	1341	1250	1324	1.20	0.5	5.95	5.99	0.97	1.44
40.9	1216 ± 57	1064	1166	1117	1291	1235	1215	0.95	0.4	5.95	5.99	0.98	1.44
43		1050	1148	1103	1275	1221	1260	1.10	0.4	5.95	5.99	0.99	1.44
43.6	1269 ± 22	1046	1144	1106	1235	1219	1257	1.10	0.3	5.82	5.70	0.80	1.40
59		960	1042	1047	1124	1130	1111	0.95	0.2	5.70	5.64	0.82	1.36
61.1	1104 ± 20	950	1030	1045	1122	1119	1119	1.00	0.2	5.68	5.63	0.83	1.36
66		928	1006	1028	1066	1091	1028	0.85	0.1	5.60	5.55	0.80	1.35
67.4	1074 ± 32	923	999	1026	1056	1087	1087	1.00	0.08	5.60	5.53	0.80	1.35
68.3	1064 ± 16	919	995	1024	1052	1082	1063	0.95	0.075	5.55	5.49	0.80	1.33
83		867	934	948	979	1015	987	0.93	0.015	5.40	5.38	0.78	1.29
84.9	981 ± 15	861	928	979	983	1008	989	0.95	0.01	5.40	5.36	0.80	1.29
95		833	895	949	952	968	956	0.97	0.01	5.40	5.28	0.79	1.29
97.2	919 ± 24	827	888	949	951	963	923	0.90	0.005	5.35	5.28	0.80	1.28